APPLICATION OF THE CALCIUM LOOPING PROCESS FOR THERMOCHEMICAL STORAGE OF VARIABLE ENERGY

KELLY ATKINSON

Thesis submitted to the University of Ottawa in partial fulfillment of the requirements for the degree of M.A.Sc in Chemical Engineering

Department of Chemical and Biological Engineering
Faculty of Engineering
University of Ottawa

Abstract

On May 11th, 2019, atmospheric CO_2 levels reached 415 ppm, a number 40% higher than the maximum level ever reached in the 800 000 years prior to the Industrial Revolution. This rise can be directly attributed to human activity, and has been linked to global temperature increase and climate change. Net CO_2 emissions continue to rise as economies grow, and in 2018 global emissions reached 37.1 Gt.

In order to reach the climate targets identified in the 2015 Paris Agreement, some scientists estimate that the world will need to attain net-zero anthropogenic greenhouse gas (GHG) emissions by 2050. Achieving this goal will require deployment of multiple technologies across multiple sectors. Of particular importance will be reducing or eliminating emissions associated to energy production via combustion of fossil fuels, which account for over 80% of CO_2 emissions in G20 countries. One method of achieving this is to displace fossil fuel electricity generation with renewable source generation. Canada currently has 12 GW of installed wind capacity, and although it is the country's fastest-growing source of renewable electricity, widespread deployment is inhibited by technical challenges including the time variability and geographic dispersion of sources.

A potential solution to overcome the challenges facing integration of renewables is grid-scale energy storage. Many storage technologies currently exist at various levels of maturity. Although currently low on the development scale, thermochemical energy storage (TCES) has gained significant interest due to its potential to offer low-cost, short- or long-term storage of high-temperature heat using non-toxic, abundant materials. Several recent works have focused on the potential to pair the calcium looping (CaL) process, which exploits the reversible calcination of calcium carbonate, with concentrated solar power (CSP). This would enable CSP to provide continuous power to the grid while receiving discontinuous solar input, and recent projects have predicted storage cycle efficiencies in the range of 38-46%.

As an extension of the work done to date, this project proposes a novel configuration of the CSP-CaL process which may offer advantages over other proposed configurations, including a reduction in process equipment requirements, elimination of pressure differentials between vessels, and a reduction in compression duty during the energy discharge period. A process simulation of the proposed system shows that it is capable of offering comparable storage cycle efficiencies, with the overall efficiency being strongly dependent on the residual conversion of calcium oxide in the carbonator as well as on the efficiencies of the power cycles employed to discharge the stored energy.

In addition to the technical challenges that may come with this type of system, social and economic barriers may arise due to the fact that it will require large-scale storage of CO_2, mining of natural limestone, and potentially large and complex facilities. All of these challenges must be considered and addressed in order to achieve deployment of this technology within Canada and around the world.

Sommaire

Le 11 mai 2019, les niveaux de CO_2 atmosphérique ont atteint 415 ppm, un nombre 40 % supérieur au niveau maximum jamais atteint au cours des 800 000 ans précédant la révolution industrielle. Cette augmentation peut être directement attribuée à l'activité humaine et a été liée à l'augmentation de la température mondiale et au changement climatique. Les émissions nettes de CO_2 continuent d'augmenter à mesure que les économies se développent et, en 2018, les émissions mondiales ont atteint 37,1 Gt.

Afin d'atteindre les objectifs climatiques identifiés dans l'Accord de Paris de 2015, certains scientifiques estiment que le monde devra atteindre zéro émission anthropique nette de gaz à effet de serre (GES) d'ici 2050. Atteindre cet objectif nécessitera le déploiement de plusieurs technologies dans plusieurs secteurs. Il sera particulièrement important de réduire ou d'éliminer les émissions associées à la production d'énergie via la combustion de combustibles fossiles, qui représentent plus de 80 % des émissions de CO_2 dans les pays du G20. Une méthode pour y parvenir consiste à remplacer la production d'électricité à partir de combustibles fossiles par une production de sources renouvelables. Le Canada dispose actuellement de 12 GW de capacité éolienne installée, et bien qu'il s'agisse de la source d'électricité renouvelable à la croissance la plus rapide du pays, son déploiement à grande échelle est entravé par des défis techniques, notamment la variabilité temporelle et la dispersion géographique des sources.

Une solution potentielle pour surmonter les défis auxquels est confrontée l'intégration des énergies renouvelables est le stockage d'énergie à l'échelle du réseau. De nombreuses technologies de stockage existent actuellement à différents niveaux de maturité. Bien qu'actuellement faible à l'échelle du développement, le stockage d'énergie thermochimique (TCES) a suscité un intérêt considérable en raison de son potentiel à offrir un stockage à faible coût, à court ou à long terme de la chaleur à haute température en utilisant des matériaux non toxiques et abondants. Plusieurs travaux récents se sont concentrés sur le potentiel de coupler le procédé de bouclage du calcium (CaL), qui exploite la calcination réversible du carbonate de calcium, avec l'énergie solaire concentrée (CSP). Cela permettrait à CSP de fournir une alimentation continue au réseau tout en recevant un apport solaire discontinu, et des projets récents ont prédit des efficacités de cycle de stockage de l'ordre de 38 à 46 %.

Dans le prolongement des travaux réalisés à ce jour, ce projet propose une nouvelle configuration du procédé CSP-CaL qui peut offrir des avantages par rapport aux autres configurations proposées, notamment une réduction des exigences en matière d'équipement de procédé, l'élimination des différences de pression entre les cuves et une réduction des puissances de compression pendant la période de décharge d'énergie. Une simulation du système proposé montre qu'il est capable d'offrir des rendements de cycle de stockage comparables, le rendement global étant fortement dépendant de la conversion résiduelle d'oxyde de calcium dans le carbonateur ainsi que des rendements des cycles de puissance utilisés pour décharger l'énergie stockée.

En plus des défis techniques qui peuvent venir avec ce type de système, des barrières sociales et économiques peuvent survenir en raison du fait qu'il nécessitera un stockage à grande échelle de CO_2, l'extraction de calcaire naturel et des installations potentiellement grandes et complexes. Tous ces défis

doivent être considérés et relevés afin de réaliser le déploiement de cette technologie au Canada et dans le monde.

Table of Contents

List of Tables

List of Figures

Nomenclature

AA-CAES	Advanced adiabatic compressed air energy storage
CAES	Compressed air energy storage
CaL	Calcium looping
$CaCO_3$	Calcium carbonate
CaO	Calcium oxide
COP21	21st Conference of the Parties
CO_2	Carbon dioxide
C_P	Heat capacity
CSP	Concentrated solar power
GHG	Greenhouse gas
HRSG	Heat recovery steam generator
HTF	Heat transfer fluid
kJ	Kilojoule
kW	Kilowatt
kWh	Kilowatt hour
LCA	Life cycle assessment
MW	Megawatt
MWh	Megawatt-hour
n	Molar flow rate
η_R	Rankine cycle efficiency
η_{RT}	Round-trip storage cycle efficiency
ρ_E	Energy density
Q	Heat
sCO_2	Supercritical carbon dioxide
TCES	Thermochemical energy storage
TES	Thermal energy storage
TGA	Thermogravimetric analysis
u_{mf}	Minimum fluidization velocity
W	Duty
y	Mole fraction

1. Introduction

Carbon dioxide (CO_2) has been identified as a greenhouse gas (GHG), and increasing atmospheric GHG levels have been linked to global climate change. At the 2015 Conference of Parties (COP21), 196 countries negotiated the Paris Agreement, with a key goal of limiting the average global temperature increase to 2°C relative to pre-industrial levels. The following year, 174 of those countries signed the agreement and began adopting it within their legal systems, committing to also pursuing efforts to further limit global temperature increase to 1.5°C. According to some scientists, this goal will require reaching net zero anthropogenic GHG emissions by sometime between 2030 and 2050 [1]. Accomplishing this ambitious goal will require dramatic reductions in GHG emissions worldwide. Although per capita emissions are decreasing in most countries, net emissions are on the rise as global economies grow, especially in China. In 2018, global CO_2 emissions rose by 2.7% relative to 2017, reaching 37.1 gigatonnes [2].

In 2004, an analysis by Pacala and Socolow hypothesized that combined implementation of 7 out of 15 deployment-ready technologies (termed "stabilization wedges") would serve to avoid catastrophic effects of increasing atmospheric CO_2 levels [3]. In 2013, Davis et al. revisited this analysis and concluded that due to lack of intervention and continuously rising CO_2 emissions, the number of stabilization wedges required had increased to 21 – and a further 10 would be required to meet a zero-emission target [4]. These "wedges" are shown in Figure 1-1. With further increases in emissions since 2013, it is certain that the climate goals identified in the Paris Agreement can only be achieved by implementing multiple technologies across multiple sectors.

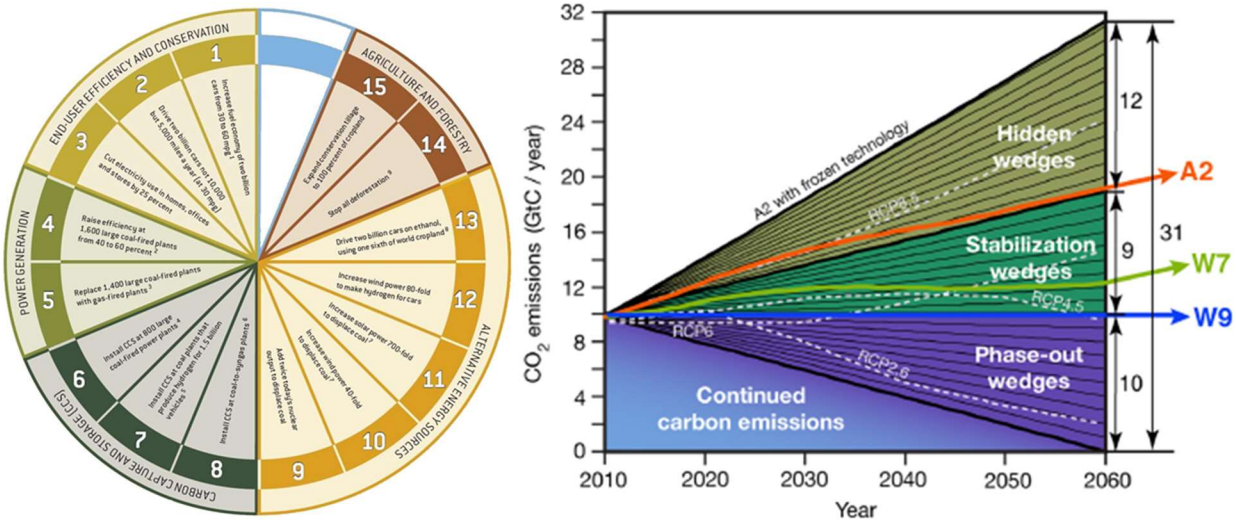

Figure 1-1: Original 15 stabilization wedges proposed by Pacala and Socolow [3], and representation of 31 wedges proposed by Davis et al [4]

Globally, over 80% of CO_2 emissions are from energy-producing combustion processes [5]. These processes include combustion of fossil fuels such as coal, oil, and natural gas for power generation and industrial processes, as well as combustion of transportation fuels such as diesel and jet fuel.

In 2018, the electricity sector in Canada contributed 9% of the country's greenhouse gas (GHG) emissions [6]. At COP21, Canada committed to reducing its GHG emissions by 30% by 2030, relative to 2005 levels [7]. In order to achieve this, a significant reduction in emissions from the electricity sector will be necessary. One method of achieving this is to displace fossil fuel electricity generation with renewable source electricity generation, such as wind and solar. One estimate is that Canada will require 100% of its electricity to come from renewables in order to meet its emissions target [8].

As of 2016, Canada has almost 17 GW of installed non-hydro renewable capacity, accounting for 11.6% of the country's electricity mix. This includes almost 12 GW of wind electricity, which is the fastest growing source of renewable electricity in Canada. In Ontario, 7.8% of electricity is generated from wind, and in Alberta its share is 6.9% [9].

Technical challenges currently inhibit the widespread deployment of renewable electricity generation. In particular, the low-density, time variability, and geographic dispersion of renewable sources make it difficult to integrate into Canada's electricity grid. Not only does this limit the ability of renewable electricity to replace fossil fuel baseload and peak-period plants, but it also leads to curtailment of renewable electricity when supply exceeds demand, negatively impacting the price of electricity [10].

This is especially true for wind energy, which is highly variable and difficult to predict [11]. This creates uncertainty for grid operators who are responsible for maintaining a stable flow of energy, and those operators must pay for facilities that are capable of quickly ramping their output to compensate for mismatches between supply and demand. Natural gas combustion turbines are commonly used to provide this reserve capacity; however, this is costly as the operator must make capacity payments to the generator, regardless of whether or not the units are operational [11]. This cost is passed on to the consumer.

1.1. Role of energy storage

A potential solution to overcome the challenges facing integration of renewables is grid-scale energy storage. This allows renewable electricity generators to store excess energy produced during low-cost off-peak periods, and deploy it to the grid during high-cost peak periods, known as energy time-shifting. This would provide capacity firming, thereby allowing the replacement of fossil-fuel peaking plants and reducing the need for curtailment. Other applications of energy storage include reserves for unexpected variations in generation and demand, frequency regulation for balancing short-term deviations, and re-energizing the grid after major outages [12]. In 2018, the global energy storage market was 12 GWh, and is expected to grow to 158 GWh by 2024 [13]

1.2. Energy storage technologies

Several storage technologies exist at various stages of development. Figure 1-2 presents a number of these technologies, and compares the product of their capital requirement and technological risk with their current maturity level [14].

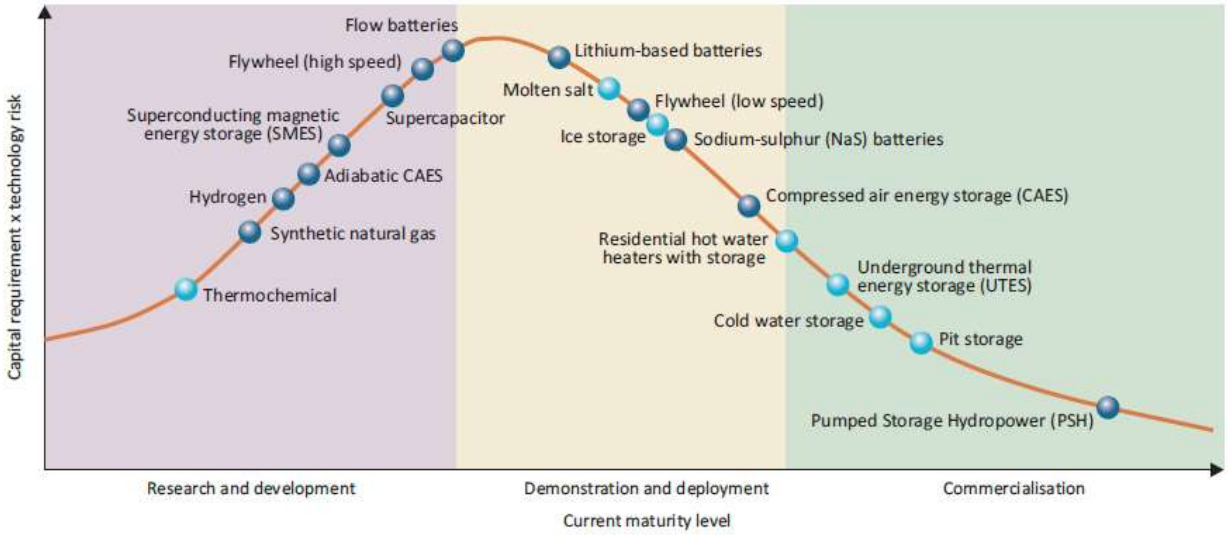

Figure 1-2: Capital requirement and technology risk of energy storage technologies at various maturity levels [14]

1.2.1. Compressed air energy storage

Compressed air energy storage (CAES) was first proposed in the 1940s and later developed in Germany in the 1960s in response to the introduction of baseload nuclear and lignite coal plants. The first CAES facility opened in 1978 in Huntorf, Germany, with a capacity of 270 MW. This was followed in 1991 by a 110 MW plant in McIntosh, Alabama. To date, these are the only two CAES plants in operation, although others are currently under development [15]

Traditional CAES consists of a series of air compressors, an air storage chamber, a combustion chamber, and a series of turbines. During the charging step, surplus electricity is used to compress air and store it at high pressure, typically in an underground geological formation. Underground storage is preferred as it minimizes surface land usage, avoids the cost of maintaining limited-size surface storage tanks, and reduces storage costs [16]. Storage chambers in existing CAES facilities operate in the range of 46-75 bar [15]. During the discharge step, compressed air is released from storage, heated in the combustion chamber via injection of natural gas, and expanded through a series of turbines [17].

The process is similar to a traditional natural gas combustion plant; however, because the compressors are driven by renewable electricity, higher turbine outputs can be achieved for a given input of natural gas [18]. Because of the design similarity to fossil fuel power plants, a CAES system coupled with a renewable energy source could act as a "renewable spinning reserve", similar to coal and gas plants which are kept running at idle speeds to reduce response time. This would enable renewable energy to replace fossil fuel peaking plants that are currently used to respond to short-term spikes in demand [16].

Due to temperature limitations on the operation of both the compressors and the storage chambers, the heat of compression must be removed from the air between compression stages and prior to storage. In traditional CAES, this heat is not recovered, resulting in an overall loss in process efficiency. Further to this, because natural gas combustion is used to heat the air before it enters the expansion turbine in the discharge step, the process results in a release of CO_2 to the atmosphere.

A schematic representation of traditional CAES is shown in Figure 1-3.

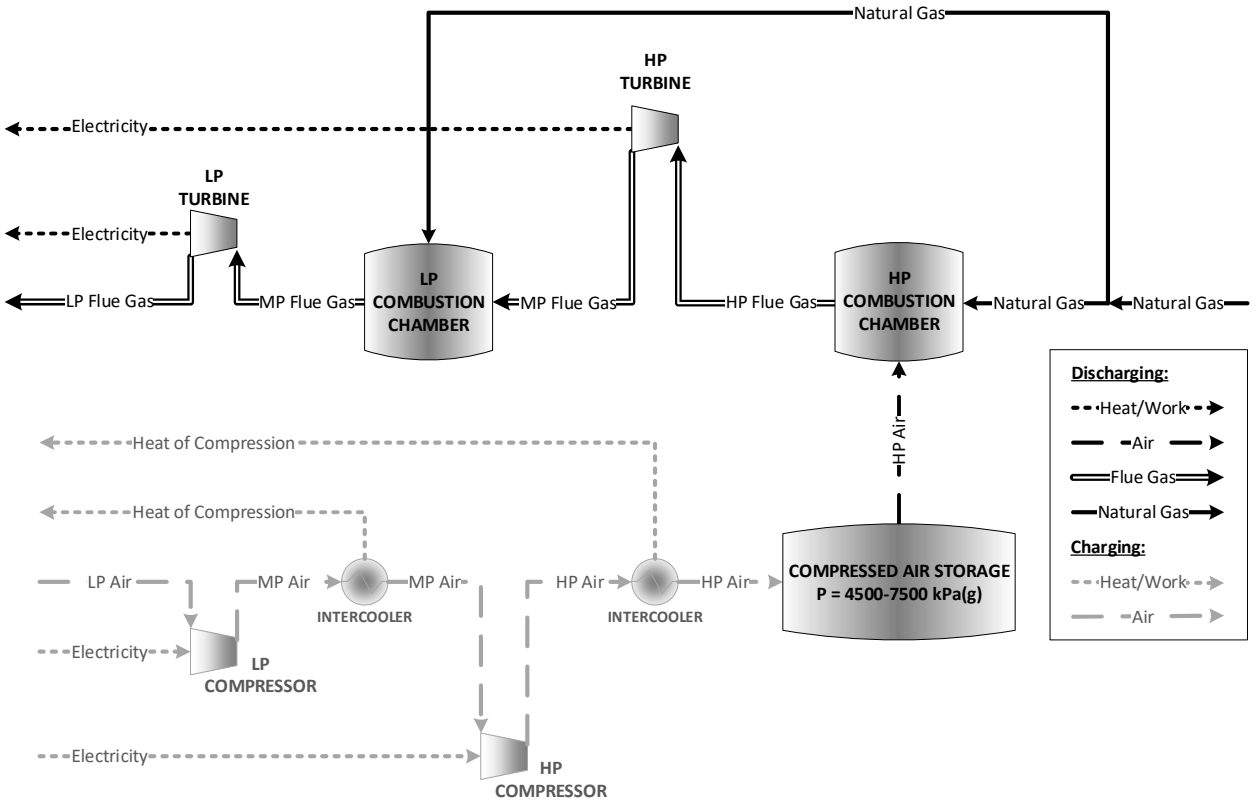

Figure 1-3: Traditional compressed air energy storage

A potential improvement to traditional CAES is advanced adiabatic CAES (AA-CAES), in which the heat of compression is stored in order to reduce efficiency losses. This can be done through a thermal energy storage (TES) system, which would be used to preheat the air before it enters the expansion turbine in the discharge step. This has the advantage of reducing or eliminating the need for natural gas, thereby reducing or eliminating CO_2 emissions and reducing the efficiency penalty represented by discharging the heat of compression to the atmosphere [19]. As shown in Figure 1-2, AA-CAES is still in the R&D phase.

A schematic representation of AA-CAES is shown in Figure 1-4.

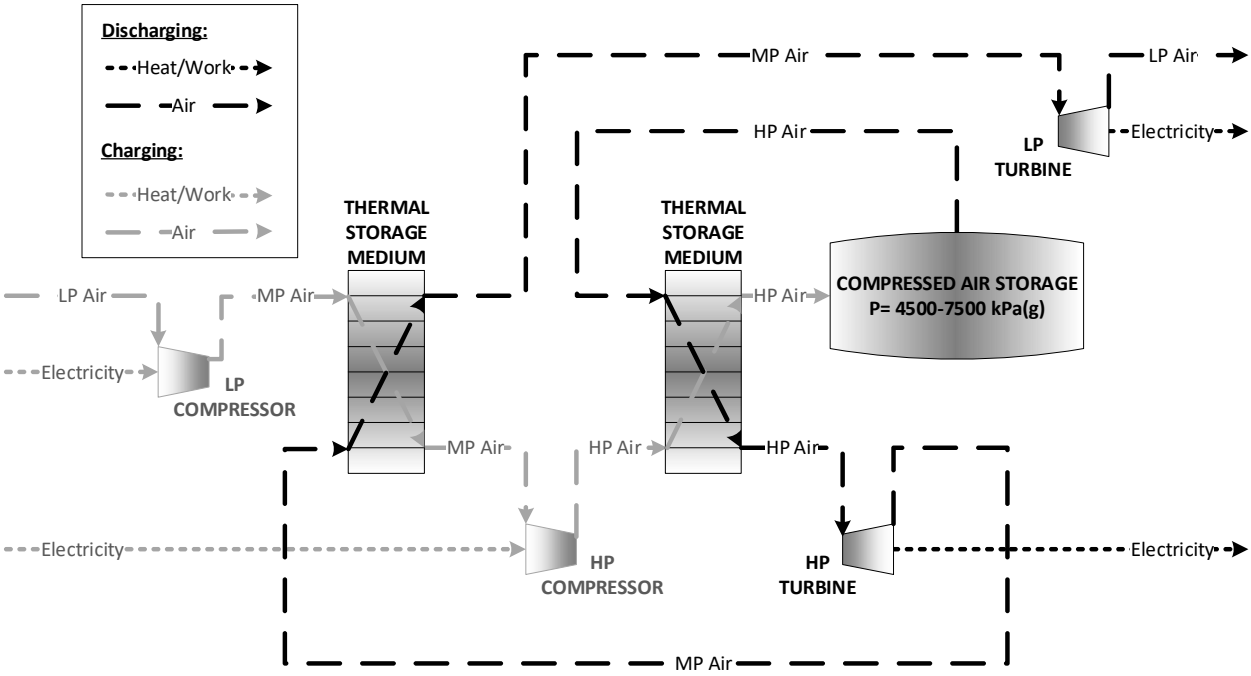

Figure 1-4: Advanced adiabatic compressed air energy storage

Potential for CAES in Canada

Ontario

CAES has been proposed as an enabling technology for integrating wind power in Ontario onto the grid [16] [11]. It could provide further service as a load-levelling technology, wherein generation is shifted from periods of low demand to periods of peak demand. A recent modelling study suggests that implementation of large-scale CAES for wind integration and load-levelling could save Ontario electricity consumers $2.5 billion over 20 years [11].

Options for reservoirs in southwestern Ontario include depleted oil and gas reservoirs and artificial caverns created through mining of salt deposits [16]. Submerged flexible storage vessels relying on hydrostatic pressure to maintain constant reservoir pressure are also an option [20].

Toronto-based technology developer Hydrostor has partnered with Toronto Hydro to demonstrate CAES at the 1 MW scale for power supply to Toronto Island, with the air being stored 60 m below the surface of Lake Ontario. This project has been operational since 2015 [20]. More recently, they have partnered with NRStor to construct a 1.75 MW CAES facility in Goderich, intended to be the world's first commercial demonstration of fuel-free CAES. It will use underground salt caverns to store the compressed air, and thermally store the heat of compression in a water storage pond to reheat the air before expansion through the turbine [11].

Alberta

As in Ontario, wind energy capacity is growing in Alberta. The potential exists for the development of CAES as there are salt caverns in the central-east and north-east regions of the province. Rocky Mountain Power Company has proposed the development of a 160 MW CAES facility in Lloydminster that would initially serve the Alberta power grid and could eventually be connected to the Saskatchewan power grid as well. This project is known as Alberta-Saskatchewan Intertie Storage (ASISt), and would be Canada's first utility-scale CAES facility [21].

1.2.2. Thermochemical energy storage

One storage technology that is low on the development curve but possesses several characteristics which may make it a valuable option is thermochemical energy storage (TCES). TCES is generally considered to be a subcategory of TES, which also includes sensible heat storage and latent heat (phase change) storage.

In comparison with sensible and latent heat storage systems, TCES has an energy density 5-10 times higher, potentially allowing for more compact energy storage. As the products of the charging reaction can be stored at ambient temperature, the storage period is theoretically unlimited, which may make it suitable for long-term energy storage [22], [23]. The cost is comparable to pumped hydro, which is at the commercialisation stage but limited by geography, and is significantly lower than flywheel storage, which is currently being deployed in Ontario [24] [25].

Several thermochemical systems have been investigated, including carbonates, hydroxides, metallic hydrides, metal oxides, ammonia, and organic. Factors to consider when choosing a suitable thermochemical system include the following [23]:

- The exothermic discharge reaction should occur at a temperature suitable for recovering high-quality heat to drive a power cycle with competitive efficiency;
- To maximize the volumetric storage capacity, a system should have large reaction enthalpy and small product volume;
- The endothermic and exothermic reactions should be completely reversible, high-yield, and produce no side products;
- The reaction rates should be sufficiently high for rapid charging and discharging; and
- The chemical compounds involved should be non-toxic, non-reactive under their storage conditions, and low-cost.

1.3. Evaluating energy storage technologies

To evaluate the suitability of a storage technology for a particular application, several metrics can be considered. These metrics include the following [25] [26]:

1. The round-trip efficiency. This is defined as the ratio of useful energy output from an energy storage system to the energy input over one duty cycle.
2. The storage capacity, in kWh.
3. The charging/discharging power, in kW.
4. The charging and discharging period. This defines the storage time scale and can indicate what time scale a storage technology may be most suitable for. It is a function of the charging/discharging power and the storage capacity.
5. The volumetric energy density, in kWh/m^3.
6. The system lifetime, measured in years or in cycles.
7. The levelized cost of energy storage (LCOES), in $/kWh, which measures the average net present cost of storage for a facility over its lifetime.
8. The environmental impact. This will include many factors, but of particular interest is the amount of CO_2 emissions that may be avoided by producing electricity from stored renewable energy instead of from fossil fuels.

In order to be competitive with other storage technologies, the proposed energy storage system (ESS) will need to outperform other technologies in one or more metrics. These metrics are available for many other storage technologies including pumped hydro, CAES, various batteries, and flywheel [28], [29].

1.4. Thesis objectives

The objectives of the proposed research are as follows:

1. Evaluate the performance of carbonates in a grid-scale thermochemical energy storage system for integration of renewable energy, on the basis of round-trip efficiency and energy storage density, for a given storage capacity and charging period. The potential benefits of integrating this storage system with compressed gas storage/CCS will be investigated, and different heat integration options will be considered.
2. Evaluate the operating limits of the proposed storage system to determine its suitability for different applications.
3. Compare the performance of the proposed energy storage system with previously proposed thermochemical systems employing carbonates.
4. Assess the preliminary implications for energy policy in Canada, taking into account key factors in the consideration of societal acceptance of thermochemical energy storage.

2. Novel configuration of an integrated thermochemical – compressed-gas energy storage system using the calcium looping process

2.1. Introduction

As described in Section 1, many energy storage technologies exist at various levels of development. Compressed air energy storage (CAES) is a viable option with projects underway in Canada, but has technical limitations in both the traditional and advanced adiabatic (AA-CAES) process configurations. These limitations may be addressed by combining compressed gas storage with a thermochemical energy storage process. Criteria for a suitable thermochemical storage material were presented in Section 1.2.2. A class of materials that may meet these criteria are carbonates. The general form of the carbonation/calcination reaction is

$$MO_{(s)} + CO_{2(g)} \leftrightarrow MCO_{3(s)} \qquad \text{Equation 2-1}$$

The reaction is driven by the system temperature and the partial pressure of CO_2, and typically occurs at temperatures above 450°C [23].

Calcium oxide and calcium carbonate, $CaO/CaCO_3$, is one such material system. The reversible reaction is as follows [30]:

$$CaO_{(s)} + CO_{2(g)} \leftrightarrow CaCO_{3(s)} \qquad \Delta H_r\,[25°C] = -178.2\ kJ/mol \qquad \text{Equation 2-2}$$

The equilibrium partial pressure of CO_2 is related to temperature as per Equation 2-3, where pressure is in bar(a) and temperature is in °C.

$$P_{eq} = 4.137 \times 10^7 e^{\left(-\frac{20474}{T+273}\right)} \qquad \text{Equation 2-3}$$

The calcium looping (CaL) process has been investigated extensively for the purpose of post-combustion CO_2 capture. It offers potential benefits in comparison to more mature CO_2 capture technologies as the projected efficiency penalty is lower (6-8% points as opposed to 8-12.5% points for amine scrubbing or oxy-combustion technologies). However, deployment of this process has been hindered in part by the tendency of natural limestone to deactivate after relatively few cycles under CO_2 capture conditions, leading to a low residual carbonation conversion [31]. Carbonation conversion is the fraction of CaO that is converted to $CaCO_3$ during the forward reaction shown in Equation 2-2. The multicycle CaO conversion can be calculated according to Equation 2-4, for example, where N is the number of calcination-carbonation cycles the sorbent has undergone, X_N is the carbonation conversion after N cycles, X_r is the residual carbonation conversion, and k is a deactivation constant [32].

$$X_N = X_r + \frac{X_1}{k(N-1) + \left(1 - \frac{X_r}{X_1}\right)^{-1}}$$ Equation 2-4

The parameters k and X_r can be determined from curve fitting to experimental data obtained via thermogravimetric analysis (TGA), with k typically increasing with more extreme calcination conditions (e.g. longer calciner residence time, higher calcination temperature) as these conditions will lead to increased sorbent sintering [33]. To mitigate the effects of sorbent deactivation, it may be necessary to implement a sorbent purge and makeup with fresh sorbent [34].

More recently, the CaL process has been investigated for integration with concentrated solar power (CSP) in order to decouple the availability of sunlight from the production of electricity (CSP-CaL). Although the current installed capacity of CSP is only about 1/10 that of photovoltaic (PV) solar power, it has some features that may lead to further deployment, including the fact that it generates high-temperature heat, making it suitable to couple with a thermochemical system with a high turning temperature such as the CaL process [35]. At the laboratory scale, extensive testing has been conducted to determine the suitability of the CaL process for TCES, with a focus on the kinetics [36] [37] and the multicyclic CaO conversion [38] [39], as these will differ under energy storage conditions as compared to post-combustion CO_2 capture conditions.

Further work has considered process integration of the CaL process with CSP technology. Edwards and Materić [40] proposed a configuration in which $CaCO_3$ is calcined in a solar calciner operating at 900°C during sun hours. The produced CaO and CO_2 are stored in order to provide a constant flow to a pressurized fluid bed carbonator operating at 875°C and 6.7 bar(g) under an air/CO_2 atmosphere. The energy released in the carbonation reaction is transferred by the air to a turbine, where electricity is generated via an open Brayton cycle. The proposed model includes heat integration to recover sensible heat from the products of both the calciner and the carbonator.

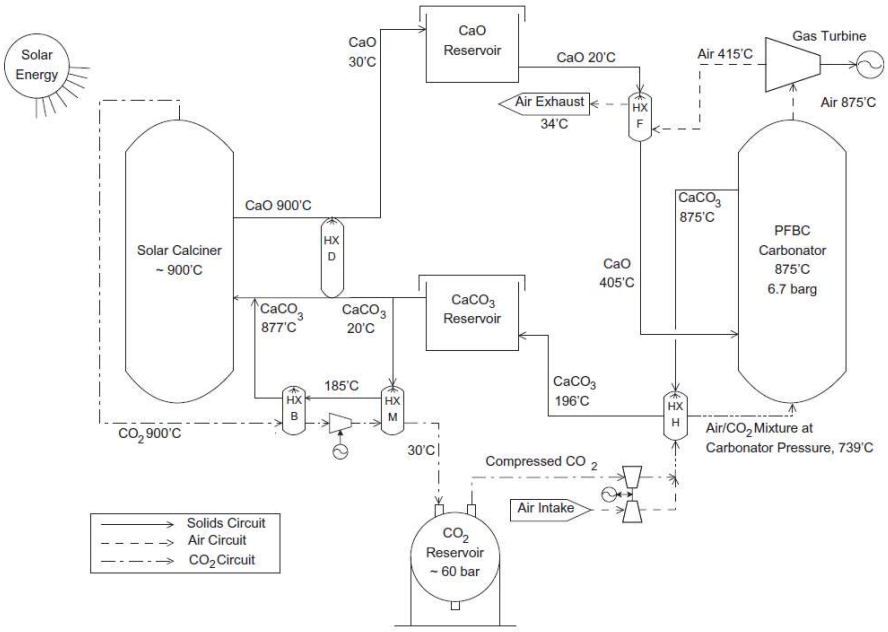

Figure 2-1: Energy storage system proposed by Edwards and Materić [40]

Results from the model indicated that the carbonator temperature and pressure, along with the activity of the solids, were critical to the efficiency of the power plant. To achieve optimum efficiency, sorbent activity greater than 15% is required, with activity between 20-40% leading to a significant reduction in capital costs. In order to provide a higher volumetric energy density than existing molten salt thermal storage systems, activity greater than 17% is required. A carbonator operating temperature between 800 and 900°C and pressure between 2.8 and 9.1 bar(g) was found to result in plant efficiencies between 40 and 46% with sorbent activity in the range of 20 to 40%.

Edwards and Materić assume in their work that all of the CO_2 supplied in the air/CO_2 stream to the carbonator will react to produce $CaCO_3$, and justify this assumption on the basis that any unreacted CO_2 would react with CaO in a subsequent direct-contact gas-solid heat exchanger. Given the thermodynamic limitation implied by Equation 2-3, it would not be possible to reach 100% CO_2 conversion, although under the right conditions it would be possible to come very close. To improve upon this, Chacartegui et al [41] proposed a configuration using a closed Brayton cycle with regeneration in which the carbonator operates under a 100% CO_2 atmosphere, thereby eliminating all CO_2 emissions to the atmosphere. This configuration includes

- A solar calciner operating at atmospheric pressure and 900°C;
- Two storage silos at atmospheric pressure for CaO and $CaCO_3$/CaO;
- A supercritical CO_2 storage vessel at 75 bar and ambient temperature;
- A low-temperature supercritical CO_2 turbine between the CO_2 storage vessel and the carbonator;
- A pressurized fluidized carbonator operating under a pure CO_2 atmosphere at 3.2 bar and 875°C; and
- A high-temperature main CO_2 turbine operating downstream of the carbonator.

A schematic diagram of this proposed configuration is shown in Figure 2-2.

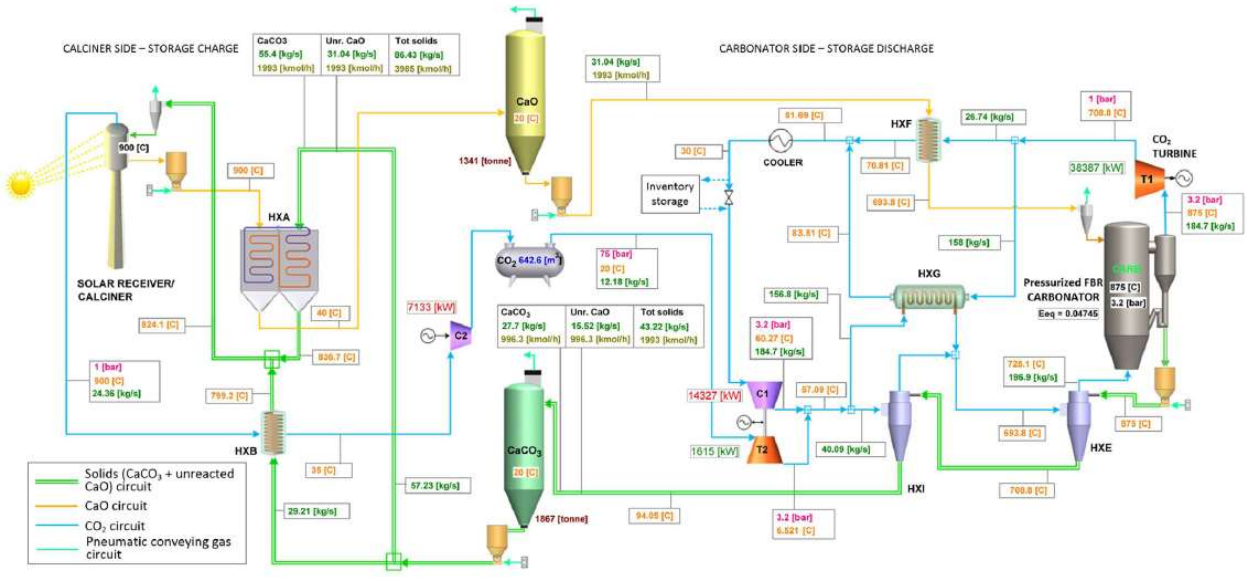

Figure 2-2: Energy storage system configuration proposed by Chacartegui et al [41]

In this process, the amount of CO_2 entering the carbonator is in significant excess to the stoichiometric amount required to react with the active CaO. This excess CO_2 absorbs the heat of carbonation and acts as the working fluid in the main CO_2 turbine. The authors used pinch analysis to optimize their process integration and studied the effects of CaO conversion, pressure ratio in the main CO_2 turbine, absolute carbonator pressure, carbonator temperature, and turbine outlet temperature on the global thermal efficiency. Their optimized integration included

- A solid-solid heat exchanger to preheat a portion of the solids entering the calciner using sensible heat from the CaO exiting the calciner;
- An indirect gas-solid heat exchanger to preheat a portion of the solids entering the calciner using sensible heat from the CO_2 exiting the calciner;
- Two direct gas-solid heat exchangers to preheat the CO_2 entering the carbonator using sensible heat from the streams exiting the carbonator;
- An indirect gas-solid heat exchanger to preheat the CaO entering the carbonator using sensible heat from a portion of the CO_2 exiting the main CO_2 turbine after the carbonator; and
- A gas-gas heat exchanger to preheat the CO_2 entering the carbonator using sensible heat from a portion of the CO_2 exiting the main CO_2 turbine after the carbonator.

As expected, results indicate that maintaining high CaO conversion is beneficial in all aspects, including efficiency, equipment size, conveying power demand, and make-up $CaCO_3$ required. The optimal pressure ratio in the main CO_2 turbine was found to be 3.2, although higher pressure ratios result in decreased heat exchanger size, particularly the gas-gas heat exchanger most impacted by the volumetric flow rate of CO_2. Because their proposed configuration includes a CO_2 expansion turbine upstream of the carbonator, the authors found that lower absolute carbonator pressures led to higher performance due to a higher

expansion ratio in this turbine. However, higher carbonator pressures allowed operation at higher temperature, which increased efficiency in the main CO_2 turbine downstream of the carbonator. Overall, results indicated that for carbonation conversion in the range of 0.07-0.7, thermal efficiencies of 39-46% could be attained without accounting for conveying solids energy consumption. Efficiencies were higher when the carbonator was operated at atmospheric pressure with turbine expansion to sub-atmospheric pressure.

Subsequent work by the same group [42] analyzes three possible configurations incorporating a closed CO_2 power cycle. The first configuration is similar to that proposed in Chacartegui et al. but without the gas-gas heat exchanger; the second configuration further eliminates one of the gas-solid heat exchangers on the carbonator side; and the third, which is found via pinch analysis to be optimal, returns to that proposed by Chacartegui et al. This layout allows high efficiencies to be obtained at significantly lower pressure ratios than in the other two layouts (PR = 3.2 instead of PR ≥ 30). In all configurations, they suggest over-expanding the CO_2 exiting the main turbine to below atmospheric pressure in order to achieve higher pressure ratios while maintaining the absolute carbonator pressure at a reasonable value. For carbonation conversion in the range of 0.5-1, they attained efficiencies of 41-47% without accounting for energy consumption due to solids conveying.

In their next work [43], the authors explore the integration of the CSP-CaL process with four different power cycles:

- A direct closed Brayton CO_2 cycle;
- A Rankine reheat cycle;
- An indirect supercritical CO_2 (sCO_2) Brayton cycle; and
- A combined closed Brayton/Rankine cycle.

The integration with a direct closed Brayton cycle closely resembles the optimized layout from their previous work. The integration with a Rankine reheat cycle transfers heat from the carbonator effluent gas to a steam cycle incorporating high- and low-pressure turbines, a main heat exchanger and a reheater, and four feedwater heaters. In the indirect sCO_2 cycle, heat is transferred from the carbonator effluent gas to supercritical CO_2 operating in a cycle incorporating a main heat exchanger, a turbine, two compressors, and two recuperators. The combined cycle, as implied, combines the first two power cycles described, with heat for the Rankine cycle being recovered downstream of the main gas turbine for the Brayton cycle. In their comparative analysis of these cycles, the authors report that the highest performance was attained with the direct closed Brayton cycle.

In a more recent work [44], the authors investigate new process schemes for CSP-CaL integration that implement high-temperature solids storage in order to simplify the heat integration. This work considers four proposed configurations:

- Case 1, a base case which includes no heat exchangers for recovery of sensible heat from solid streams exiting the calciner and carbonator (but includes a gas-gas heat exchanger to transfer heat from the CO_2 exiting the carbonator to the CO_2 entering the carbonator);

- Case 2, which incorporates a gas-solid heat exchanger to transfer sensible heat from the CO_2 exiting the calciner to the solids entering the calciner, and two gas-solid heat exchangers to transfer sensible heat from the solids exiting the carbonator to the CO_2 entering the carbonator;
- Case 3, which uses an intercooled main CO_2 compressor and increases heat exchange in the gas-gas exchanger, thereby decreasing overall electricity consumption in the process; and
- Case 4, which uses the same configuration as Case 3 but operates the carbonator at atmospheric pressure.

Each of these configurations includes power generation on the calciner side via recovery of sensible heat from the CO_2 stream exiting the calciner in a heat recovery steam generator and superheated steam cycle. For the selected pressure ratio of 3 and carbonation conversion of 0.2, the maximum storage cycle efficiency achieved is 38.1% and occurs for both Case 3 and Case 4. This efficiency accounts for energy consumption due to solids conveying. Selecting between Cases 3 and 4 would require analysis of the benefits of eliminating the lock hoppers for solids pressurization/depressurization vs. requiring larger equipment to handle larger gas volumes as well as achieving a lower reaction rate in the carbonator. Further, the authors conclude that selecting an optimum configuration would require a techno-economic analysis to assess the benefits of decreasing the technical complexity of a CSP-CaL plant vs. achieving higher efficiencies.

Most recently, Ortiz et al have proposed a configuration in which a combined cycle, consisting of a CO_2 turbine and a heat recovery steam generator (HRSG), operates continuously. This configuration is shown in Figure 2-3. CO_2 is employed as a heat transfer fluid (HTF) in a closed loop on both the calciner and carbonator sides of the process. During daylight operation, the HTF is heated in a solar receiver and circulated through a heat exchanger in the calciner, driving the calcination reaction, before being circulated to the combined cycle. During night operation, the HTF is circulated through a heat exchanger in the carbonator and heated by the carbonation reaction before being circulated to the combined cycle. The calciner is operated at atmospheric pressure and the carbonator is operated at 8 bar in order to have similar operating temperatures between the two reactors. The authors report an overall plant efficiency of 44.5% [45].

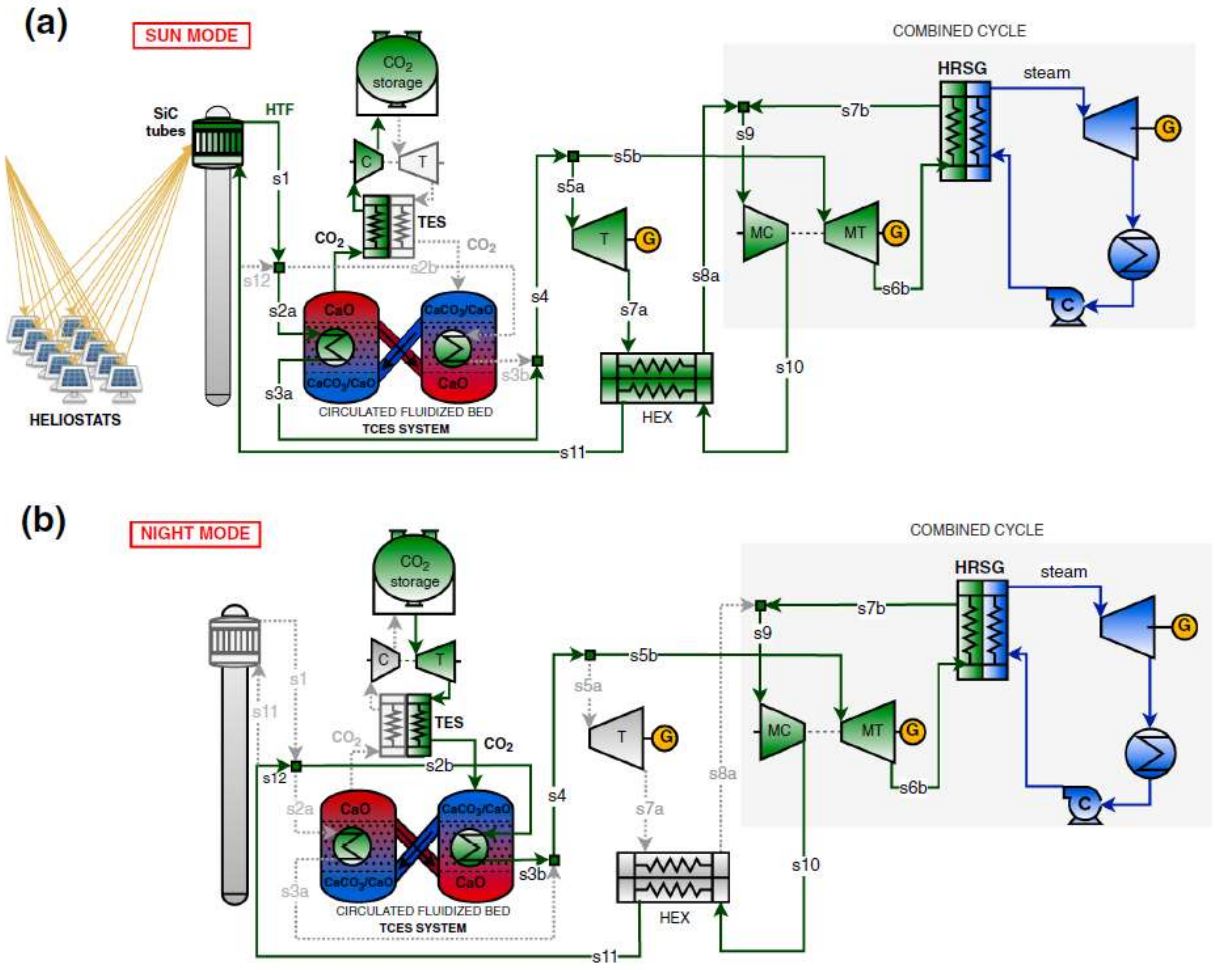

Figure 2-3: Conceptual scheme of novel configuration proposed by Ortiz et al [45]

Other work has considered the calcium looping process as a method to both decarbonise coal-fired electricity and increase power generation flexibility through energy storage [46].

When considering the work that has been done to this point on integrating the calcium looping process with a CSP plant, it can be noted that with the direct CO_2 Brayton cycle integration schemes proposed, the pressure ratio in the main turbine is intrinsically linked to the absolute carbonator operating pressure. As a result, it is necessary to either operate the carbonator above atmospheric pressure or induce a vacuum at the turbine outlet in order to achieve an optimal pressure ratio. Operating the carbonator at elevated pressure necessitates the use of lock hoppers to transfer solids to and from the carbonator and the atmospheric calciner, in some cases at high temperature, which increases the technical complexity as well as the capital and operating costs. Further, in some cases the CO_2 stream exiting the carbonator may contain entrained solids that will need to be separated from the gas stream to the level of tolerance in the turbine. Solids removal equipment will entail additional complexity, as well as heat losses that will reduce the overall efficiency of the storage system.

2.2. Proposed energy storage system description

As an extension of the work that has been done to date, a configuration which decouples the carbonator pressure from the turbine pressure, enables atmospheric pressure operation of both the carbonator and the calciner, and supplies a stream of clean CO_2 to a turbine is proposed. This configuration further draws upon work done to develop AA-CAES technology and stores energy both thermochemically and mechanically by compressing the CO_2 produced in the calciner. This presents an advantage over AA-CAES in that heat to the gas entering the main turbine is supplied from a thermochemical process rather than thermal storage, meaning that longer storage duration may be feasible.

For the purposes of comparison with similar systems being proposed, energy input to the calciner is coming from CSP, and the carbonator is operated continuously with the calciner operating for 12h in a 24h period. However, the process configuration would be suitable for storing energy derived from any source operating at sufficiently high temperature to drive the calcination reaction. This could potentially include storing energy coming directly from the electricity grid via electrical heating in a fluidized bed calciner. A process flow diagram of the proposed system is presented in Figure 2-4, followed by a process description.

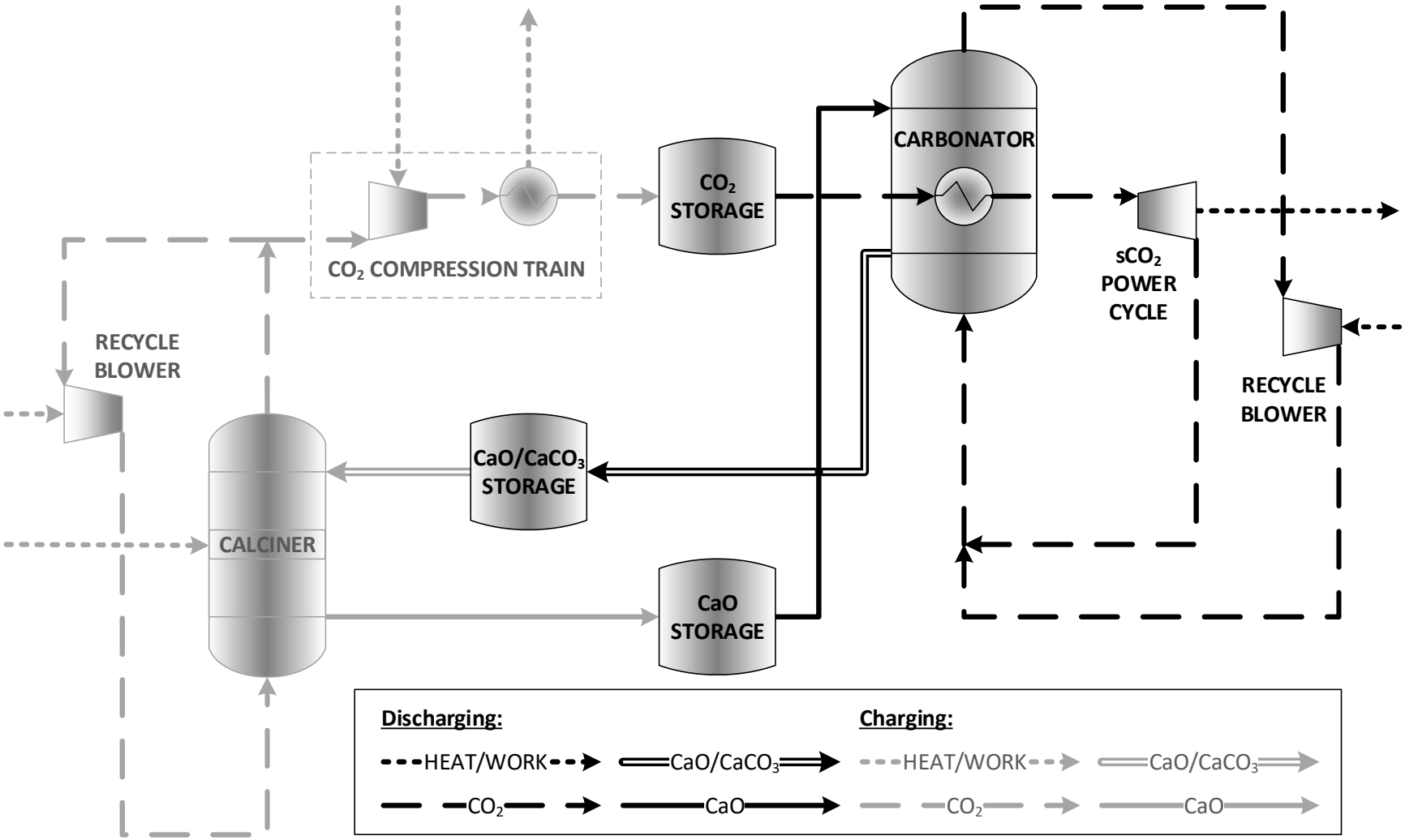

Figure 2-4: Basic process flow diagram of proposed energy storage system

CO_2 is stored under supercritical conditions at 7500 kPa(g) and ambient temperature in the CO_2 storage tank, while CaO is stored at atmospheric pressure in the CaO storage tank. CaO enters the carbonator, where it undergoes a carbonation reaction with CO_2 to produce $CaCO_3$, as per Equation 2-2. The produced $CaO/CaCO_3$ stream is then sent to storage in the $CaO/CaCO_3$ storage tank. The unreacted CO_2 exits the carbonator and is recycled back to provide continuous fluidization.

The carbonation reaction supplies heat to the supercritical CO_2 (sCO_2) via an in-bed heat exchanger, which then enters an sCO_2 power cycle. CO_2 exits the power cycle and is combined with the CO_2 exiting the recycle blower and recycled to the carbonator. The carbonator operates continuously to provide a constant power output over a 24h period.

On the calciner side, $CaO/CaCO_3$ exits the storage vessel and enters the calciner where the $CaCO_3$ in the stream undergoes calcination to produce CaO and CO_2. The CaO exits the calciner and enters the CaO storage vessel. The calciner operates over a 12h period, with mass and molar flow rates on the calciner side being double those on the carbonator side.

CO_2 exits the calciner and is split between being recycled to the calciner via the recycle blower and being sent to the CO_2 compression train. It exits the compression train and enters the CO_2 storage vessel.

2.3. Process model

2.3.1. Model assumptions

To assess the relative merits of the proposed storage system, a process model was built in Aspen HYSYS V11. The following assumptions can be applied to all scenarios considered in this work:

1. The $CaCO_3$ in the stream entering the calciner undergoes complete decomposition to produce CaO and CO_2.
2. The calciner operates as a falling particle or fluidized bed, with gas velocity at the inlet being equal to the minimum fluidization velocity (u_{mf}) and gas velocity at the outlet being $1.1u_{mf}$, with the difference in velocity being due to the evolution of CO_2 within the reactor.
3. The calciner operates isothermally at the equilibrium temperature calculated using Equation 2-3.
4. The carbonator operates as a falling particle bed, with gas velocity being equal to $1.1u_{mf}$ at the inlet and equal to u_{mf} at the outlet, with the difference being due to consumption of CO_2 within the reactor.
5. The carbonator operates isothermally at 20°C below the equilibrium temperature calculated using Equation 2-3, in order to maintain the driving force for carbonation while minimizing required heat exchange surface areas.
6. The round trip efficiency of the process is calculated over a 24-hour period.
7. Gas/solid and gas/liquid heat exchangers have a minimum approach temperature of 15°C.
8. Solid/solid heat exchangers have a minimum approach temperature of 20°C.
9. Utility cooling water is available at 20°C.
10. Ambient temperature is 20°C.

11. Compressors have an adiabatic efficiency of 89%.
12. Turbines have an isentropic efficiency of 75%.
13. CaO has a particle density of 2000 kg/m^3.
14. $CaCO_3$ has a particle density of 2800 kg/m^3.
15. Solids (CaO, $CaCO_3$, and mixtures) have an average bed void fraction of 0.4.

2.3.2. Unit operations

Although full design of unit operations is outside the scope of this work, consideration has been given to the different equipment options currently available at the commercial scale, as well as options that are currently under development.

Calciner

Calcination is a commercial technology used in cement production. Reactors currently used in this application are rotary kilns capable of operating at up to 2000°C and producing around 3600 tons/day of CaO. Traditionally, heat is supplied to drive the calcination reaction via fossil fuel combustion. These reactors provide the necessary conditions for calcination to occur, including

- sufficient residence time for particles to reach reaction temperature and undergo full calcination;
- high heat transfer coefficients; minimal thermal gradients; and
- mechanisms for prevention of particle attrition and agglomeration [47].

Although not yet commercial for CaL applications, other reactor types that can provide similar conditions include fluidized bed reactors and entrained flow reactors, which have been studied for application in both CO_2 capture and energy storage applications.

A variety of fluidized bed technologies, as well as falling particle receivers and centrifugal particle receivers, have been proposed for CSP-CaL applications, and an extensive review on the state-of-the-art is provided by Tregambi et al [35] [47]. The majority of the work thus far has been conducted at the laboratory scale. The SOLPART project, which ran from 2015-2019, moved the concept of solar calcination to the pilot scale. It was conducted with the goal of developing and implementing a high-temperature solar process for thermal treatment of particles, such as the calcination of limestone in the cement industry, to eliminate the need for combustion of fossil fuels for heat. Although this project does not have an energy storage component, their work on modelling and designing solar calciners will be significant to the continued development of CSP-CaL technology [48] [49].

Carbonator

The conditions required for carbonation are similar to those required for calcination, with the distinction that longer residence times are required in order for CaO particles to reach their residual conversion values. Most carbonators proposed for CO_2 capture applications are fluidized bed reactors, although entrained flow reactors are being studied for both CO_2 capture and energy storage applications [47].

Power cycles

Steam Rankine cycles have been fundamental to the power industry for close to a century. The cycle efficiency is dependent on the steam temperature and pressure. Modern high-efficiency steam plants utilize supercritical steam at up to 25 000 kPa(g) and 565 °C, and typically have efficiencies in the range of 42-44%. Facilities employing sub-critical cycles typically operate in the 38-42% efficiency range. Although many programs around the world are working to develop cycles that can exceed 50% efficiency, this will require a major step forward in technology, as currently-used materials cannot be used at temperatures and pressures higher than those already achieved [50].

The supercritical CO_2 (sCO_2) Brayton cycle has gained attention in recent years for application in power industries including nuclear, solar, and fossil fuel. It naturally lends itself to integration with a CaL process, as CO_2 can be both a reactant and working fluid. Compared to a steam Rankine cycle, sCO_2 is less corrosive at similar temperatures, requires 10x smaller turbomachinery due to the high fluid density beyond the critical point, and can offer a thermal efficiency up to 5% higher. However, the turbine pressure ratio is smaller than in a steam Rankine cycle, leading to a relatively high turbine outlet temperature. This means that the thermal efficiency is highly dependent on the recovery of heat at the turbine outlet. A variety of layouts incorporating heat recuperation have been studied, with a recompression cycle leading to the highest efficiency [51].

Storage vessels and solids handling equipment

Storage vessels are required for the CaO and CO_2 streams exiting the calciner, as well as for the mixed $CaO/CaCO_3$ stream exiting the carbonator. Ideally, these storage vessels should be as small as possible to reduce capital costs, with smaller storage tanks expected in comparison with current molten salts-based solar power plants due to the higher storage density provided by the CaL process [47]. If hot solids storage is implemented, the vessels will require insulation to minimize heat losses and increase overall process efficiency.

Handling of hot solids can add significant complexity to a power plant, especially in a case where there is the potential for solids to be under a reactive environment, as is the case with the CaL process. Options for conveying equipment include both mechanical systems and pneumatic systems, both of which include established technology options used in many applications. Mechanical systems typically have a higher investment cost but lower operating cost in comparison with pneumatic systems. Other important factors to consider are the ability of the equipment to avoid particle segregation by size and to maintain a low energy consumption [47].

Heat exchangers

Heat exchangers are essential to the proposed process in order to maximize use of sensible heat and thus maximize the overall process efficiency. Depending on the storage scenario being considered, the process may require both gas-solid and solid-solid heat exchangers. Gas-solid heat exchangers may be either direct or indirect, depending on the stream compositions and temperatures, in order to avoid unintended carbonation in heat exchange equipment. While different types of solid-solid heat exchangers have been

proposed, including an indirect configuration employing a heat transfer fluid in direct contact with both solids streams, this equipment is not developed on a commercial scale [47].

2.3.3. Storage scenarios

To optimize the energy storage process, four possible configurations for implementing heat integration are considered based on the desired storage tank temperatures. The desired storage tank temperatures will depend on the intended storage duration. These configurations can be summarized as follows:

Configuration 1: Heat is recovered from the solids exiting the carbonator and used to power a supercritical steam cycle. Heat is not recovered from the solids exiting the calciner; these solids are stored at high temperature. This configuration is considered most applicable under short storage duration, where heat loss from stored solids will be minimal.

Configuration 2: Heat is recovered from the solids exiting the carbonator and used to power a supercritical steam cycle. Heat is recovered from the solids exiting the calciner and used to pre-heat a portion of the solids entering the calciner. This configuration is considered most applicable under long storage duration, where heat loss from stored solids would be significant.

Configuration 3: Heat is not recovered from the solids exiting the carbonator or from the solids exiting the calciner; all solids are stored at high temperature. This configuration is considered most applicable under short storage duration, where heat loss from stored solids will be minimal.

Configuration 4: Heat is not recovered from the solids exiting the carbonator. Heat is recovered from the solids exiting the calciner and used to pre-heat a portion of the solids entering the calciner.

In this work, Configurations 1 and 2 are modelled to assess their applicability in short- and long-term storage scenarios. Configuration 3 may be competitive with Configuration 1 from a thermodynamic perspective, and should be considered for future work. On the other hand, Configuration 4 is not expected to be beneficial under any circumstance due to the fact that it inherently places heat recovery on the calciner side rather than on the carbonator side, i.e. during the charging period rather than during the discharging period, and is therefore not considered for further work.

It should be noted that in Configurations 1 and 3, in which solids are stored hot under a CO_2 atmosphere, there is the potential for carbonation reactions to continue outside of the reactors – for example, in the conveying lines or in the storage vessels. This is considered in the analysis of Configuration 1.

Configuration 1

Configuration 1 was developed to enable a direct comparison of the technical merits of the storage system with that proposed by the University of Seville. A process flow diagram for this configuration is shown in

Figure 2-5. In this case, the calciner operates over a 12-hour period and the carbonator over a 24-hour period, meaning that material flow rates on the calciner side of the process are twice those on the carbonator side of the process, with the storage vessels acting as a buffer between the two sides. To maximize heat extraction on the carbonator side, solids exiting the calciner are not cooled but instead are stored hot, with heat loss from the storage tank being accounted for. Solids exiting the carbonator side have heat extracted in heat exchangers HX-L and HX-O, with this high-temperature heat being used to drive a supercritical steam power cycle in order to maximize power production.

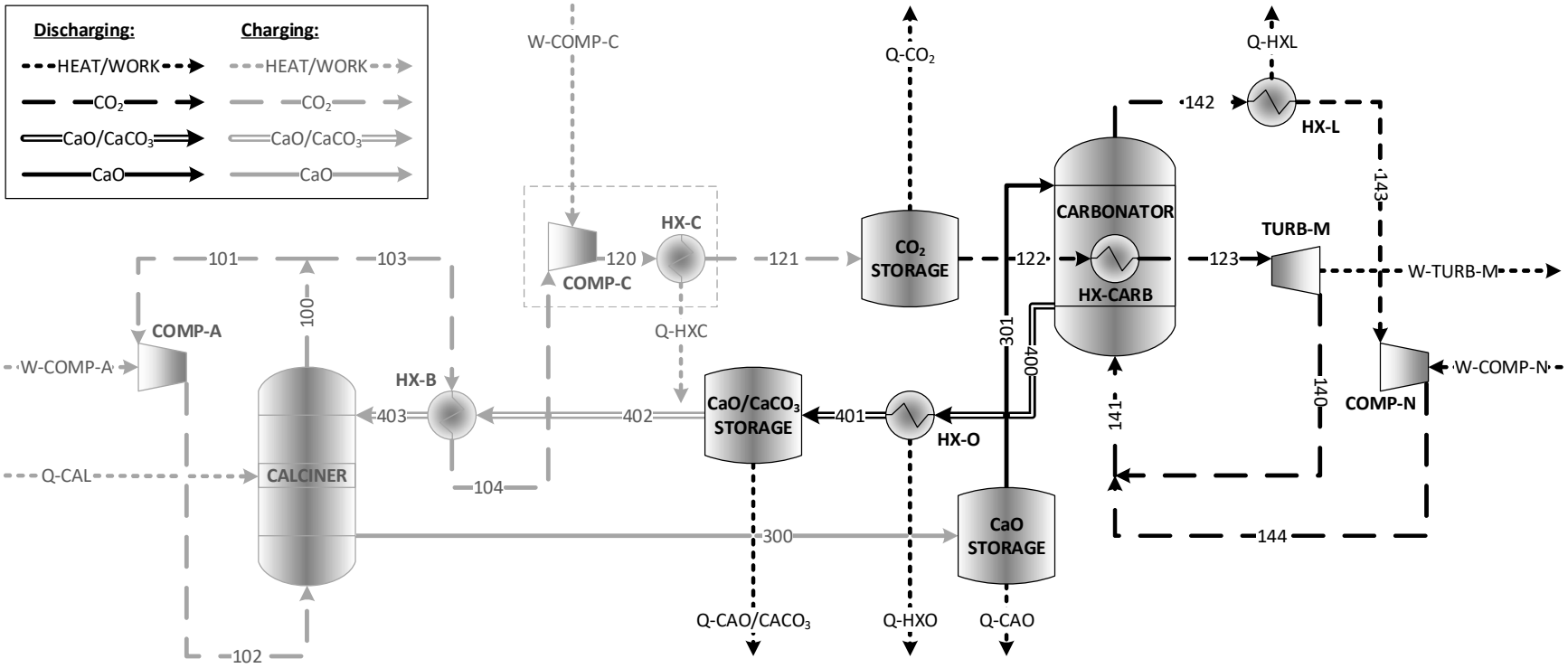

Figure 2-5: Process flow diagram for Configuration 1; Hot CaO storage and cold $CaO/CaCO_3$ storage

A summary of base case inputs to the process model for Configuration 1 is presented in Table 2-1. The power input to the calciner is used as the baseline for the assessment and is equal to 100 MW, or 3.6×10^8 kJ/h. The calciner is operated at the equilibrium temperature predicted by Equation 2-3 for a system operating at atmospheric pressure. The carbonator is operated at 20°C below this equilibrium temperature in order to enable the carbonation reaction to proceed while minimizing heat transfer surface areas.

The main CO_2 compressor, represented in Figure 2-5 as COMP-C and HX-C, is modelled as a multi-stage compressor with a maximum stage outlet temperature of 150°C and interstage cooling provided by utility cooling water. This yielded a 4-stage compressor with each stage having a pressure ratio of 2.9. A fraction of the heat of compression is recovered to preheat Stream 402 before it enters HX-B, with the maximum temperature of this stream being fixed at 15°C below the highest-temperature stream exiting a compression stage in COMP-C.

The round-trip storage cycle efficiency, η_{RT}, can be calculated according to Equation 2-5:

$$\eta_{RT} = \frac{24h \cdot [W_{TURB-M} + \eta_R \cdot (Q_{HX-O} + Q_{HX-L})]}{12h \cdot [Q_{CAL} + W_{COMP} \quad + W_{COMP-} \ ] + 24h \cdot W_{COMP-}} \qquad \text{Equation 2-5}$$

Here, W_{TURB-M} is the work produced in the main turbine, in MW; Q_{HX-O} and Q_{HX-L} are the heat produced in heat exchangers HX-O and HX-L, respectively, in MW; Q_{CAL} is the heat input to the calciner, in MW; W_{COMP-A}, W_{COMP-C}, and W_{COMP-N} are the duties of compressors COMP-A, COMP-C, and COMP-N, respectively, in MW, and η_R is the efficiency of a steam Rankine cycle.

The energy storage density, ρ_E, measured in GJ/m^3, can be calculated according to Equation 2-6:

$$\rho_E = \frac{Q_{CAL}}{V_{CaO} + V_{CaO/CaCO_3} + V_{CO_2}} \qquad \text{Equation 2-6}$$

Here, V_{CaO} is the volume required to store the CaO exiting the calciner, in m^3; $V_{CaO/CaCO3}$ is the volume required to store the CaO/$CaCO_3$ exiting the carbonator, in m^3; and V_{CO2} is the volume required to store the CO_2 exiting the calciner, in m^3.

Configuration 2

Configuration 2 was developed for scenarios in which long-term storage is required and would lead to unfavourably high heat loss from stored solids. A process flow diagram for this configuration is presented in Figure 2-6. Heat recovery is maximized during both charging and discharging stages through addition of heat exchangers HX-D and HX-P. The recovery of heat in HX-P leads to lower-temperature heat being available from HX-O in comparison with Configuration 1; this heat is used to drive a subcritical steam power cycle

Analysis of Configuration 2 resulted in the observation that above a carbonator CaO conversion of approximately 0.42, recovery of heat in HX-P led to an excess of heat available on the carbonator side. To continue the analysis beyond this conversion limit, a modified version of Configuration 2 was developed in which HX-P is replaced by a cooler, HX-Q, allowing for additional power generation on the carbonator side. This modification is shown in Figure 2-7. Heat is recovered in HX-Q at a sufficiently high temperature to drive a supercritical steam power cycle. HX-Q is placed upstream of the recycle blower, COMP-N, to minimize the blower inlet temperature.

The energy storage density for Configuration 2 can be calculated using Equation 2-6, as with Configuration 1. The round-trip storage cycle efficiency can be calculated using Equation 2-7, and for the modified version of Configuration 2, Equation 2-8 is used which includes the heat recovered in HX-Q, denoted as $Q_{HX\text{-}Q}$, in MW

$$\eta_{RT} = \frac{24h \cdot [W_{TURB} \quad + \eta_R \cdot Q_{HX-O}]}{12h \cdot [Q_{CAL} + W_{COMP-A} + W_{COMP-C}] + 24h \cdot W_{COMP-N}} \qquad \text{Equation 2-7}$$

$$\eta_{RT} = \frac{24h \cdot [W_{TURB-M} + \eta_R \cdot (Q_{HX-O} + Q_{HX-Q})]}{12h \cdot [Q_{CAL} + W_{COMP-A} + W_{COMP-C}] + 24h \cdot W_{COMP-N}} \qquad \text{Equation 2-8}$$

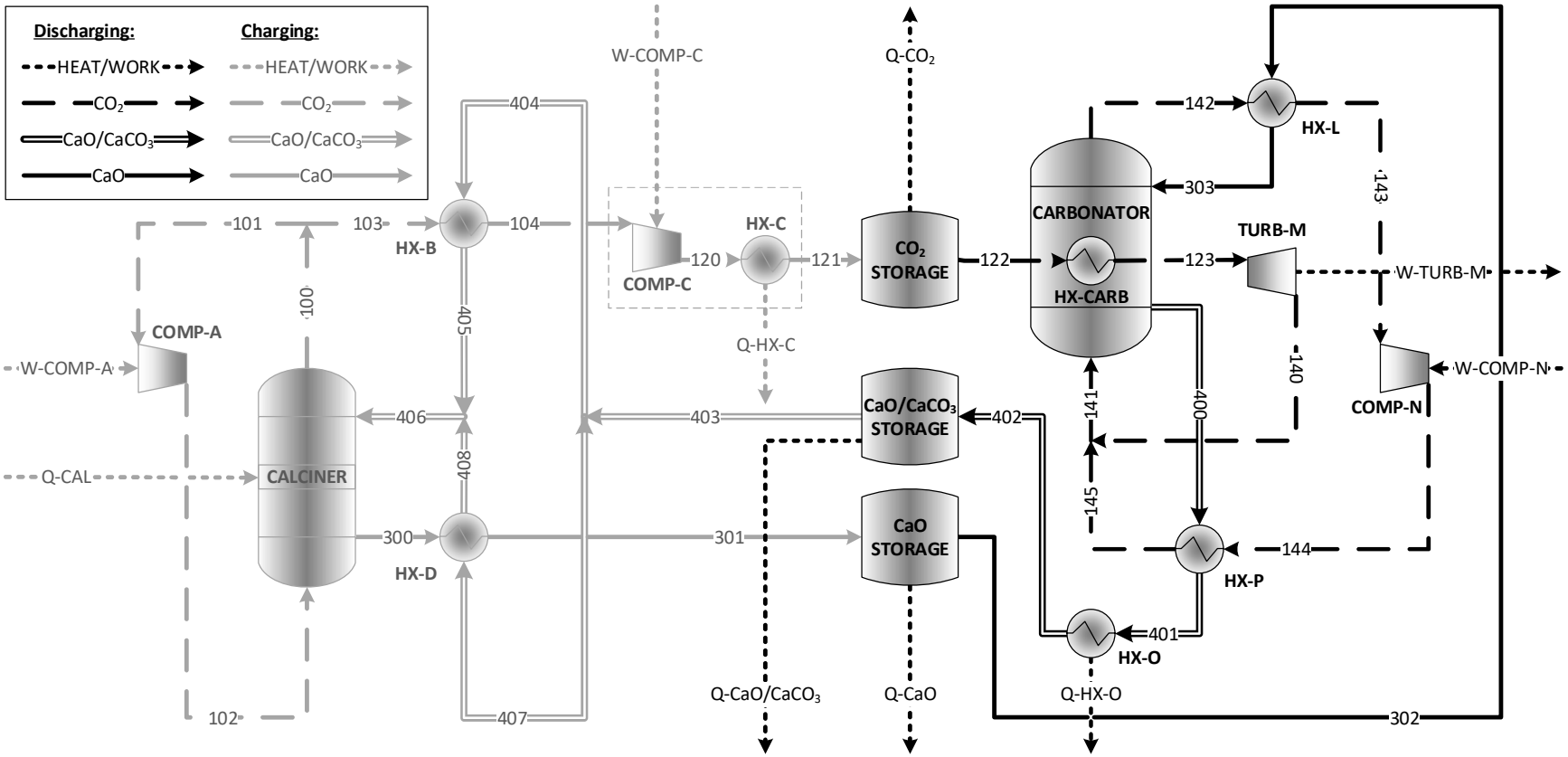

Figure 2-6: Process flow diagram for Configuration 2; Cold CaO storage and cold $CaO/CaCO_3$ storage

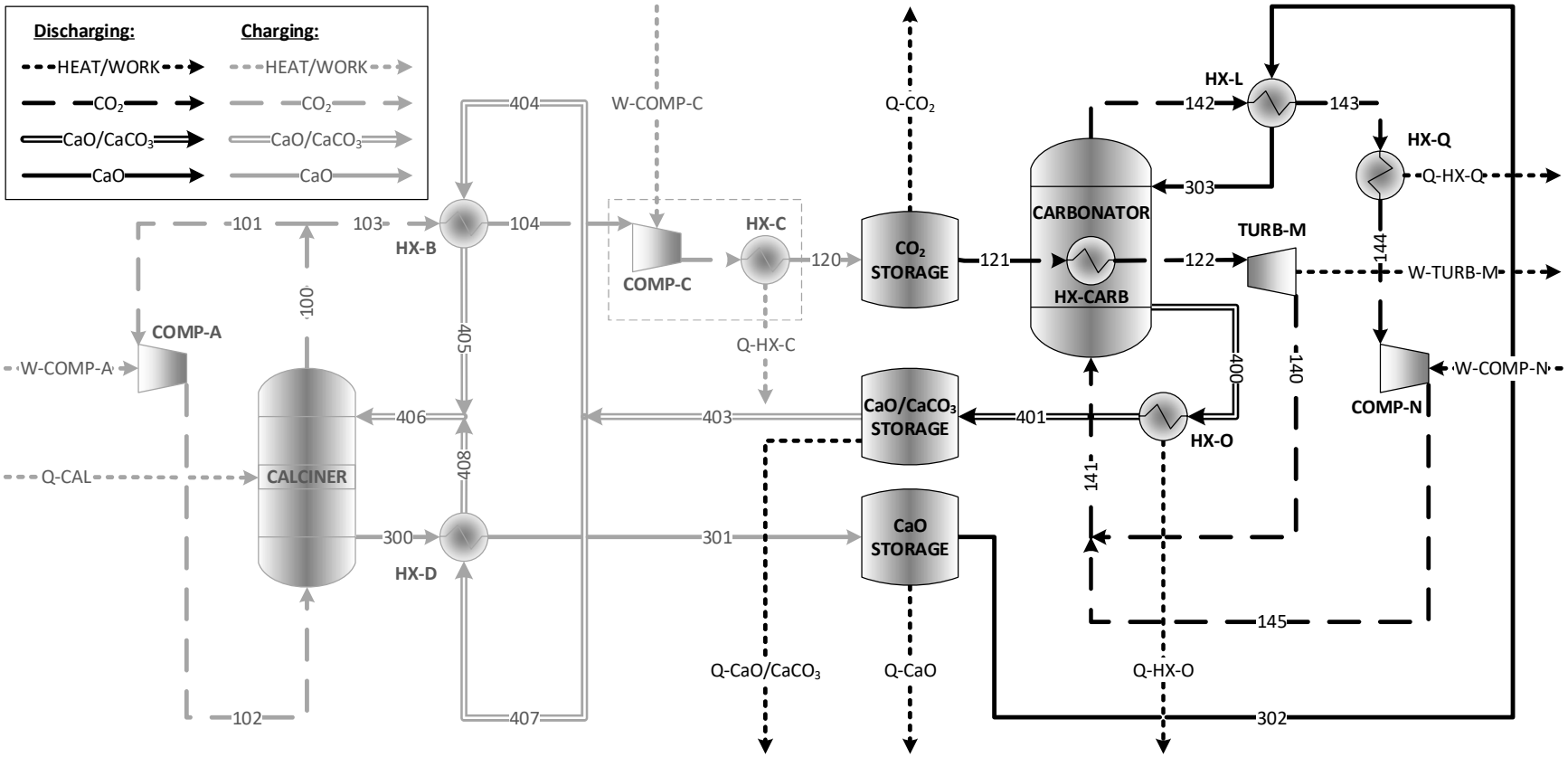

Figure 2-7: Process flow diagram for modified Configuration 2

As with Configuration 1, the main CO_2 compressor, is modelled as a multi-stage compressor with a maximum stage outlet temperature of 150°C and interstage cooling provided by utility cooling water, yielding a 4-stage compressor with each stage having a pressure ratio of 2.9. A fraction of the heat of compression is recovered to preheat Stream 403 before it is split between HX-B and HX-D. At lower conversions, this heat recovery is limited by the temperature of Streams 405, 406, and 408, which can't exceed 880°C in order to prevent calcination occurring upstream of the calciner. At higher conversions, the reduced flow rate of Stream 403 means the quantity of heat recovered is again limited to 15°C below the highest-temperature stream exiting a compression stage in COMP-C.

Table 2-1: Summary of base case process conditions for Configuration 1

Parameter	Units	Value
Power Input to Calciner	kJ/h	3.60×10^8
Calciner Operating Period (Charging Time)	h	12
Calciner Operating Temperature	°C	900
Calciner Operating Pressure	kPa(g)	10
Carbonator Operating Temperature	°C	880
Carbonator Operating Pressure	kPa(g)	10
Carbonator Operating Period (Discharging Time)	h	24
Fractional CaO Conversion in Carbonator	-	0.2
CO_2 Storage Temperature	°C	35
CO_2 Storage Pressure	kPa(g)	7500
Maximum CO_2 Compressor Outlet Temperature	°C	150
CaO Storage Temperature	°C	900
CaO Storage Heat Loss Rate	°C/h	5
$CaO/CaCO_3$ Storage Temperature	°C	35
Turbine Inlet Temperature	°C	600
Turbine Inlet Pressure	kPa(g)	7500
Turbine Outlet Pressure	kPa(g)	10
Supercritical Steam Cycle Efficiency	%	40
Subcritical Steam Cycle Efficiency	%	35
Stream Temperature Required to Drive Supercritical Steam Cycle	°C	600
Ambient Temperature	°C	20

2.4. Simulation results

2.4.1. Configuration 1

A summary of material and energy streams for Configuration 1 is presented in Table 2-2 and Table 2-3.

Table 2-2: Configuration 1 base case material stream summary

Stream ID	Stream Description	Flow Rate [kmol/h]	Flow Rate [kg/h]	Temperature [°C]
100	CO_2 exiting calciner	10 856	477 752	900
101	CO_2 entering calciner recycle blower	9 869	434 320	900
102	CO_2 entering calciner	9 869	434 320	922
103	Hot CO_2 to compression	987	43 432	900
104	Cooled CO_2 to compression	987	43 432	35
120	CO_2 entering storage	987	43 432	35
121	CO_2 exiting storage	987	43 432	20
122	Hot sCO_2 entering turbine	987	43 432	600
140	CO_2 exiting turbine	987	43 432	236
141	CO_2 entering carbonator	11 660	513 153	791
142	CO_2 exiting carbonator	11 167	491 437	880
143	CO_2 entering carbonator recycle blower	11 167	491 437	793
144	CO_2 exiting carbonator recycle blower	11 167	491 437	813
300	CaO exiting calciner	4 934	276 707	900
301	CaO entering carbonator	4 934	276 707	840
400	$CaO/CaCO_3$ exiting carbonator	2 467	160 071	880
401	Cooled $CaO/CaCO_3$ entering storage	2 467	160 071	35
402	$CaO/CaCO_3$ exiting storage	4 934	320 142	117
403	Preheated $CaO/CaCO_3$ entering calciner	4 934	320 142	262

Table 2-3: Configuration 1 base case energy input and recovery summary

Stream ID	Stream Description	Heat Flow [10^8 kJ/h]
Q-CAL	Heat input to calciner	3.60
W-COMP-A	Calciner recycle blower duty	0.12
W-COMP-C	CO_2 compressor duty	0.13
Q-HXO	Heat recovered from solids exiting carbonator	1.33
Q-HXL	Heat recovered from CO2 exiting carbonator	0.54
W-TURB-M	Main CO_2 turbine duty	0.09
W-COMP-N	Carbonator recycle blower duty	0.13

Effect of CaO conversion in carbonator

A sensitivity analysis was conducted on the effect of CaO conversion in the carbonator on the round-trip efficiency over a 24-hour period. CaO conversions between 0 and 0.7 were studied, based on the maximum CaO conversion obtained by Sànchez Jiménez et al [52]. The efficiency of the supercritical steam cycle operating with the heat extracted in HX-L and HX-O was varied from 35-45%, based on conventional and state-of-the-art steam cycle efficiencies [50]. Results of this sensitivity analysis are presented in Figure 2-8.

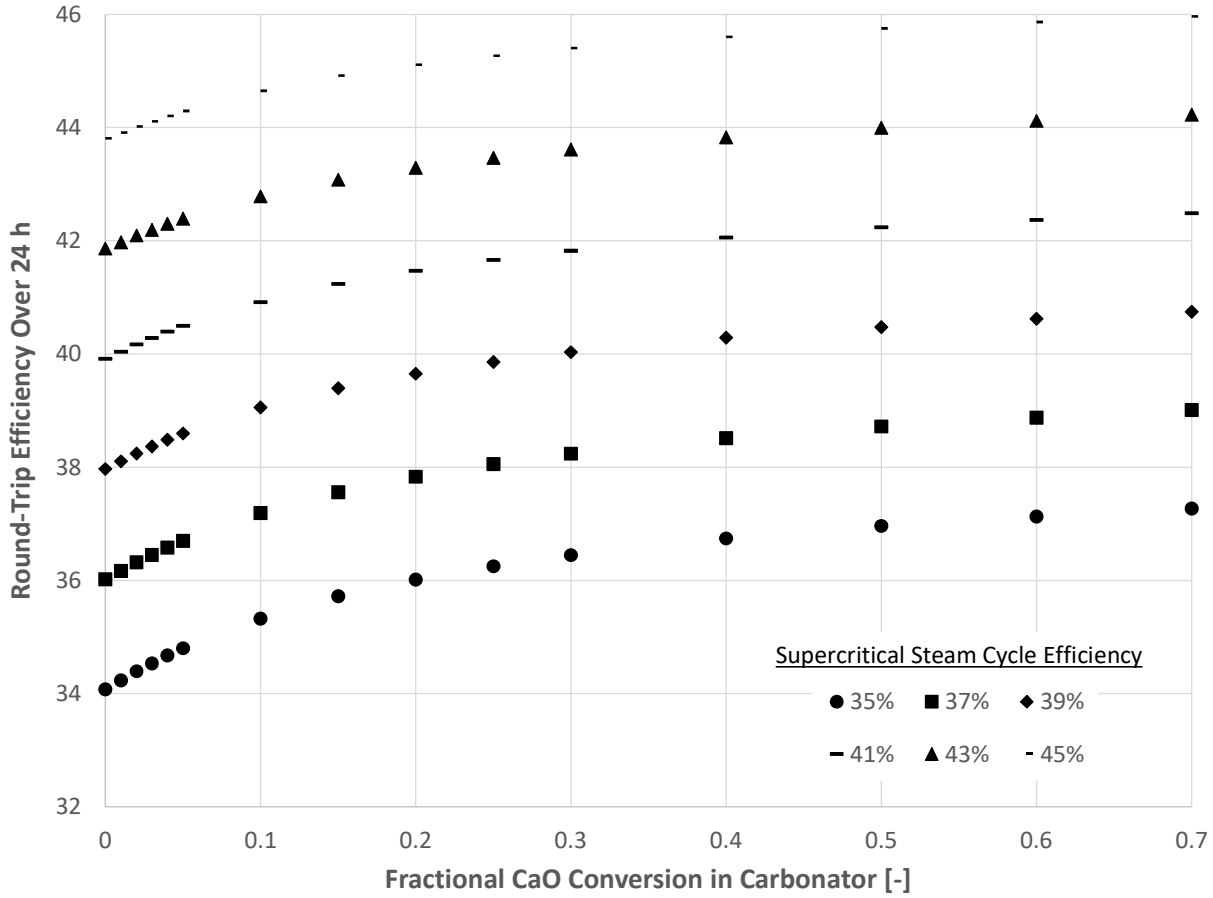

Figure 2-8: Round-trip efficiency as a function of CaO conversion for Configuration 1

As shown, for a given steam cycle efficiency, the round-trip efficiency increases by 2-3% over the given range of CaO conversion. The influence of steam cycle efficiency is more marked, with a 2% increase in steam cycle efficiency leading to an approximately 2% increase in round-trip efficiency. At the base case condition of a fractional conversion equal to 0.2, going from 35% to 45% steam cycle efficiency increases the round-trip efficiency from 36% to almost 46%.

The impact of steam cycle efficiency reflects the fact that the amount of power being produced in the steam cycle dominates the power being produced in the sCO_2 cycle. This reflects the fact that the majority of the energy entering the process is stored via the thermochemical reaction rather than via compression of CO_2. This is shown in Figure 2-9, which plots the ratio of power produced in the sCO_2 cycle to power produced in the steam cycle as a function of CaO conversion in the carbonator. As shown, increasing the conversion in the carbonator increases the net power being produced in the sCO_2 cycle; however, even at a conversion of 0.7, the ratio only reaches 0.17-0.22, depending on the steam cycle efficiency.

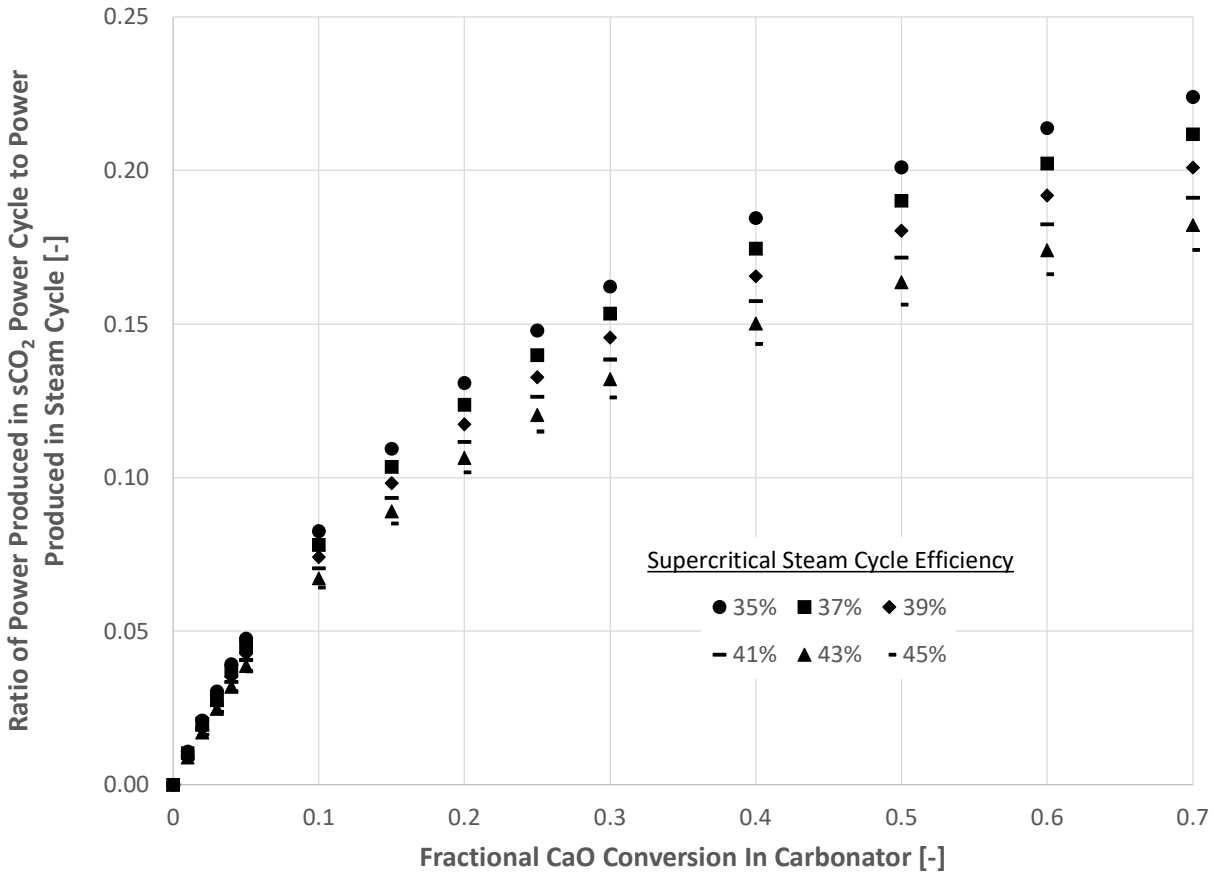

Figure 2-9: Ratio of power produced in sCO_2 power cycle to power produced in steam cycle as a function of CaO conversion for Configuration 1

The effect of CaO conversion on the amount of solids circulating in the process, and thus the required storage volume, was also investigated. Results are presented in Figure 2-10.

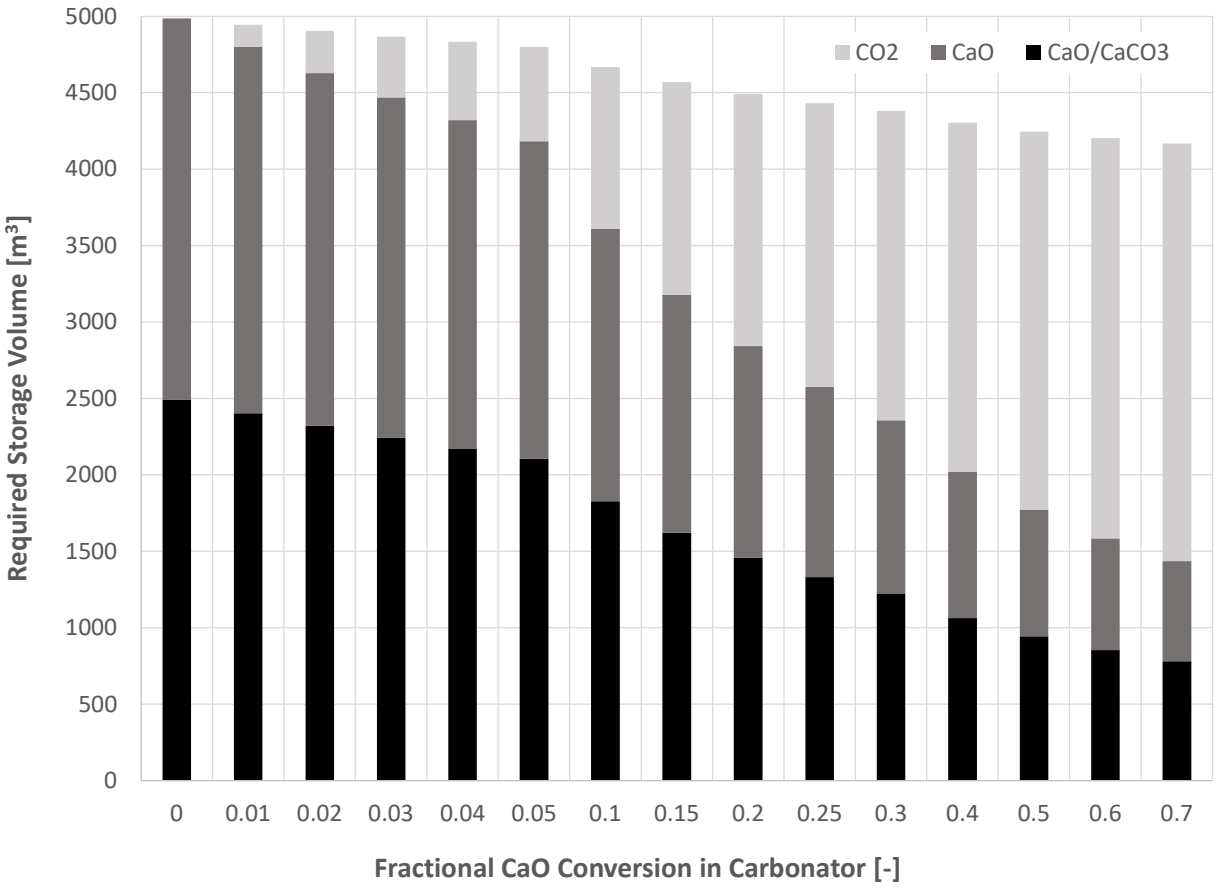

Figure 2-10: Effect of CaO conversion on required $CaO/CaCO_3$ storage volume for Configuration 1

As shown, the required storage volume decreases with increasing conversion as a result of decreasing quantity of solids. The heat supplied to the calciner is split between sensible heating of the entering solids and the heat of calcination required to convert $CaCO_3$ to CaO, as defined by Equation 2-9:

$$Q_{CAL} = \dot{n}_{403}\left[y_{CaCO3,403}C_{p,CaCO3} + \left(1 - y_{CaCO3,403}\right)C_{p,CaO}\right]\Delta T + \dot{n}_{403}y_{CaCO3,403}\Delta H_R \qquad \text{Equation 2-9}$$

Here, Q_{CAL} is the quantity of heat supplied to the calciner in kJ/h; n_{403} is the molar flow rate of solids entering the calciner in kmol/h; $C_{p,CaCO3}$ and $C_{P,CaO}$ are the heat capacities of $CaCO_3$ and CaO, respectively, in kJ/kmol°C, $y_{CaCO3,403}$ is the fraction of $CaCO_3$ in stream 403 entering the calciner; ΔT is the temperature rise from the calciner inlet to the calciner operating temperature in °C; and ΔH_R is the heat of calcination in kJ/kmol. As suggested by the second term Equation 2-9, when Q_{CAL} is held constant, increasing $y_{CaCO3,403}$ will necessarily lead to a decrease in n_{403}. As the quantity of solids circulating in the system decreases, so does the required storage volume.

Effect of sCO_2 turbine inlet temperature

A sensitivity analysis was conducted on the inlet temperature to TURB-M, the sCO_2 turbine on the carbonator side. Temperature was varied from 600 to 750°C, based on typical and advanced operating temperatures of sCO_2 power cycles [41].

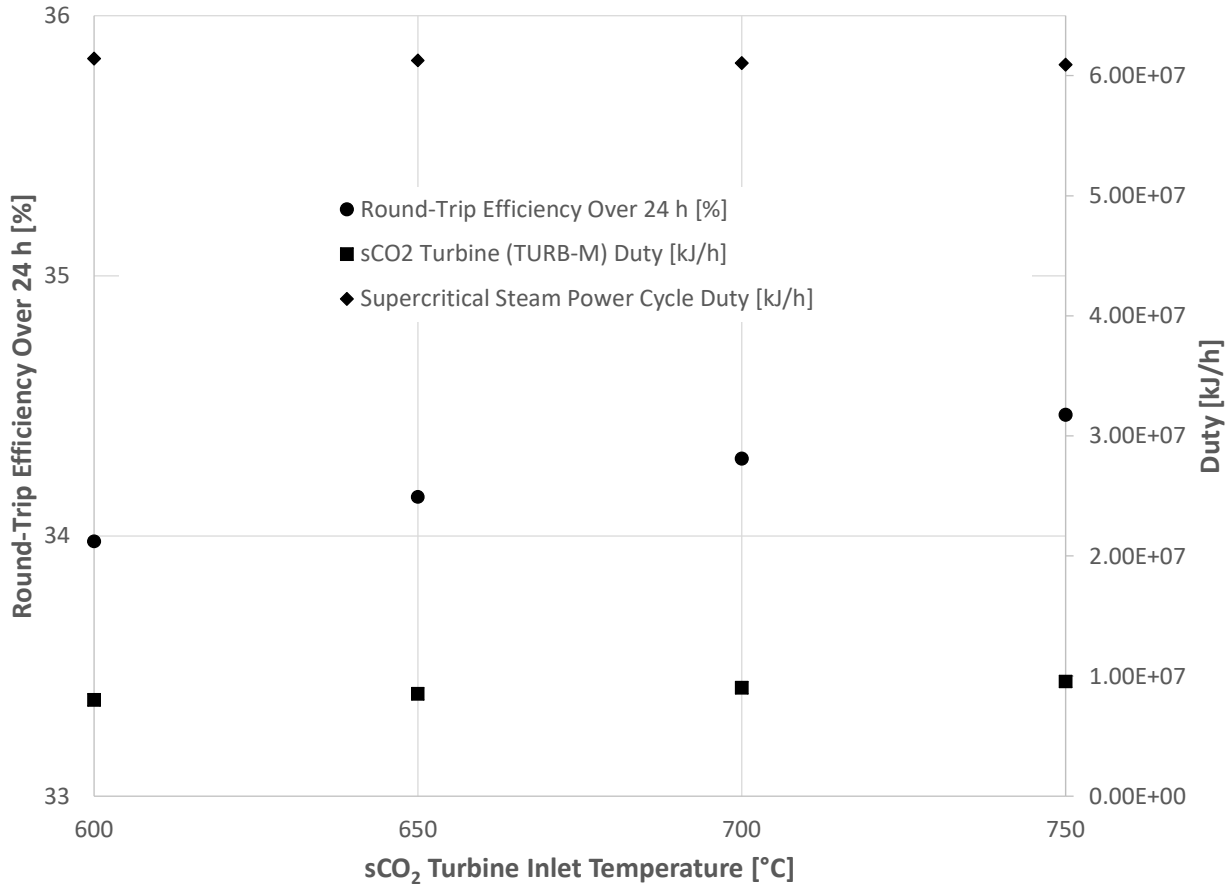

Figure 2-11: Round-trip efficiency and power cycle duty as a function of sCO_2 turbine inlet temperature

As a result of the power production ratio shown in Figure 2-9, increasing the inlet temperature of the sCO_2 turbine has a minimal impact on round-trip efficiency, with a temperature increase of 150°C leading to an efficiency increase of only 0.5%. This is because increasing the sCO_2 turbine inlet temperature, while increasing the power produced by the sCO_2 turbine, decreases the amount of heat available to be extracted in HX-L, thereby decreasing the power produced by the supercritical steam cycle. The slight net increase can be attributed to a higher cycle efficiency in the sCO_2 turbine than in the supercritical steam cycle; however, the overall impact of increasing the sCO_2 turbine inlet temperature is simply to shift where in the process power is being extracted with the majority still being via the steam cycle.

Effect of average heat loss rate in storage vessels

As shown in Figure 2-5, heat is not recovered from the CaO stream exiting the calciner (Stream 300); instead, this stream is stored at high temperature. Heat loss can be expected to occur during the 12-hour

storage period. Figure 2-12 shows the impact of the average heat loss rate on the round-trip cycle efficiency.

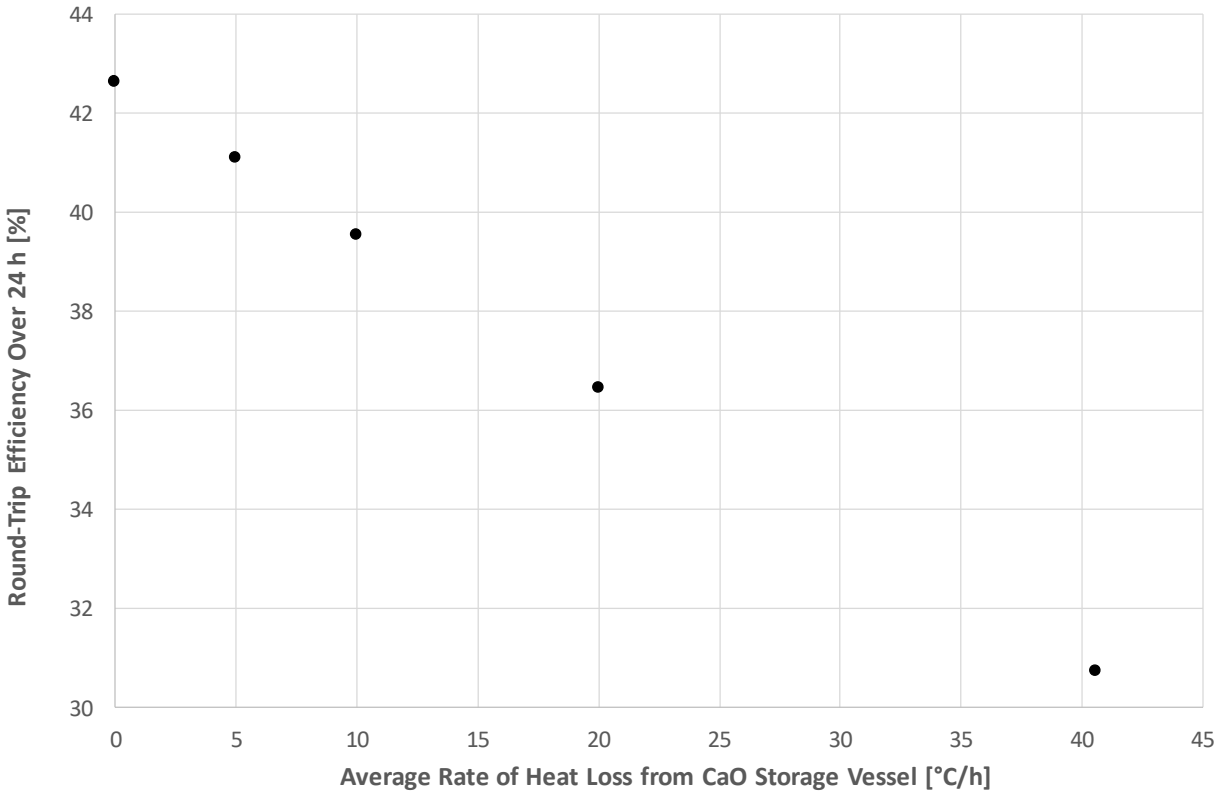

Figure 2-12: Storage cycle efficiency as a function of heat loss rate for Configuration 1 assuming a 12 h storage period

The range of average heat loss rates shown correspond to Stream 301 entering the carbonator at 900°C, i.e. no heat loss occurs, down to Stream 301 entering the carbonator at 20°C, i.e. the contents of the storage vessel reach ambient temperature. As shown, the average rate of heat loss has a significant impact on round-trip efficiency, with a decrease in round-trip efficiency of almost 12% points occurring over this range. The point at which it becomes beneficial to use Configuration 2 instead of Configuration 1 is examined in the next section.

2.4.2. Configuration 2

A summary of material and energy streams for Configuration 2 is presented in Table 2-4 and Table 2-5.

Table 2-4: Configuration 2 base case material stream summary

Stream ID	Stream Description	Flow Rate [kmol/h]	Flow Rate [kg/h]	Temperature [°C]
100	CO_2 exiting calciner	24 785	1 090 765	900
101	CO_2 entering calciner recycle blower	22 531	991 604	900
102	CO_2 entering calciner	22 531	991 604	922
103	Hot CO_2 to compression	2 253	99 160	900
104	Cooled CO_2 to compression	2 253	99 160	35
120	CO_2 entering storage	2 253	99 160	35
121	CO_2 exiting storage	2 253	99 160	20
122	Hot sCO_2 entering turbine	2 253	99 160	600
140	CO_2 exiting turbine	2 253	99 160	236
141	CO_2 entering carbonator	11 660	513 153	661
142	CO_2 exiting carbonator	10 533	463 573	880
143	CO_2 entering carbonator recycle blower	10 533	463 573	446
144	CO_2 exiting carbonator recycle blower	10 533	463 573	461
145	Reheated CO_2	10 533	463 573	702
300	CaO exiting calciner	11 266	730 921	900
301	CaO entering storage	11 266	730 921	35
302	CaO exiting storage	5 633	315 877	20
303	CaO entering carbonator	5 633	315 877	865
400	$CaO/CaCO_3$ exiting carbonator	5 633	315 877	880
401	Partially cooled $CaO/CaCO_3$	5 633	315 877	538
402	$CaO/CaCO_3$ entering storage	5 633	315 877	35
403	$CaO/CaCO_3$ exiting storage	5 633	315 877	20
404	$CaO/CaCO_3$ to HX-B	1 811	117 498	59
405	$CaO/CaCO_3$ from HX-B	1 811	117 498	880
406	Preheated $CaO/CaCO_3$ entering calciner	11 266	631 754	88
407	$CaO/CaCO_3$ to HX-D	9 455	613 422	59
408	$CaO/CaCO_3$ from HX-D	9 455	613 422	880

Table 2-5: Configuration 2 base case energy input and recovery summary

Stream ID	Stream Description	Heat Flow [10^8 kJ/h]
Q-CAL	Heat input to calciner	3.60
W-COMP-A	Calciner recycle blower duty	0.28
W-COMP-C	CO_2 compressor duty	0.30
Q-HXO	Heat recovered from solids exiting carbonator	1.72
W-TURB-M	Main CO_2 turbine duty	0.20
W-COMP-N	Carbonator recycle blower duty	0.09

Effect of CaO conversion in carbonator

A sensitivity analysis was conducted on the effect of CaO conversion in the carbonator on the round-trip efficiency over a 24-hour period. CaO conversions between 0 and 0.7 were studied, based on the maximum CaO conversion obtained by Sànchez Jiménez et al [52]. The efficiency of the subcritical steam cycle was varied from 30-40%, based on conventional and state-of-the-art steam cycle efficiencies [50]. The efficiency of the supercritical steam cycle was held constant at the base case condition of 40%. Results of this sensitivity analysis are presented in Figure 2-13.

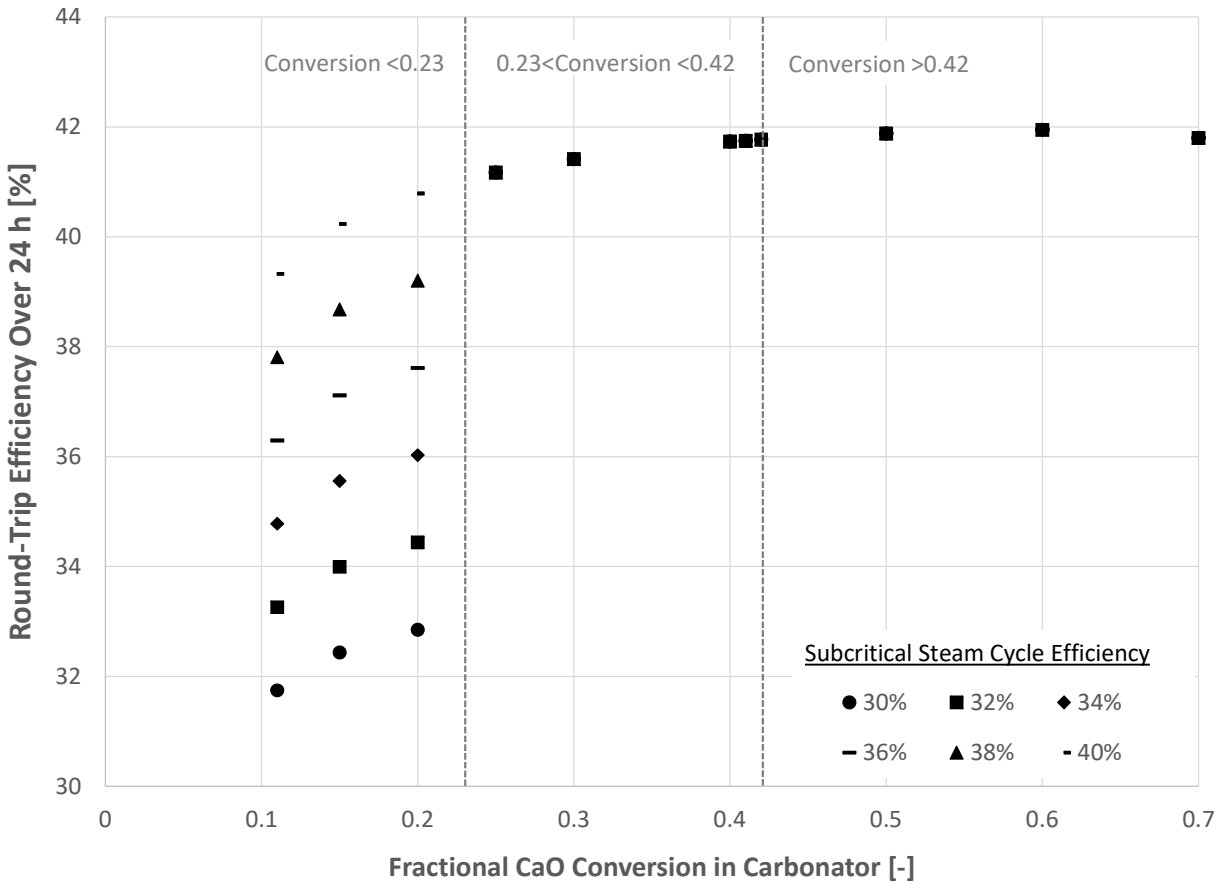

Figure 2-13: Storage cycle efficiency as a function of fractional CaO conversion in carbonator for Configuration 2

For Configuration 2, resolution of the heat balance on the carbonator side can only be attained at a carbonation conversion of 0.11 or higher. Below this conversion, Stream 144 is too cold to be sufficiently preheated in HX-P.

As shown in Figure 2-13, there are two discontinuities in the round trip efficiency. The first occurs at a carbonation conversion of 0.23. At this conversion, the temperature of Stream 401 exceeds 600°C, making it possible for the heat extracted in HX-O to drive a supercritical steam cycle instead of a subcritical steam cycle. As noted, the efficiency of the supercritical steam cycle has been fixed at 40% for the purpose of this analysis. The second discontinuity occurs at a carbonation conversion of 0.42 and is due to the production of additional power in HX-Q. Interestingly, although the quantity of heat being extracted in HX-Q increases with conversion as a result of a lower duty on HX-L and thus higher temperature at Stream 143, the overall efficiency reaches an optimum and then begins to decrease slightly with increasing conversion. This is likely because as the conversion increases, the mass flow of Stream 400 decreases, leading to less heat being available for extraction in HX-O.

The effect of CaO conversion on the amount of solids circulating in the process, and thus the required storage volume, was also investigated. Results are presented in Figure 2-14. As shown, the required

storage volume decreases with increasing conversion as a result of decreasing quantity of solids. This trend follows the same explanation provided for Configuration 1.

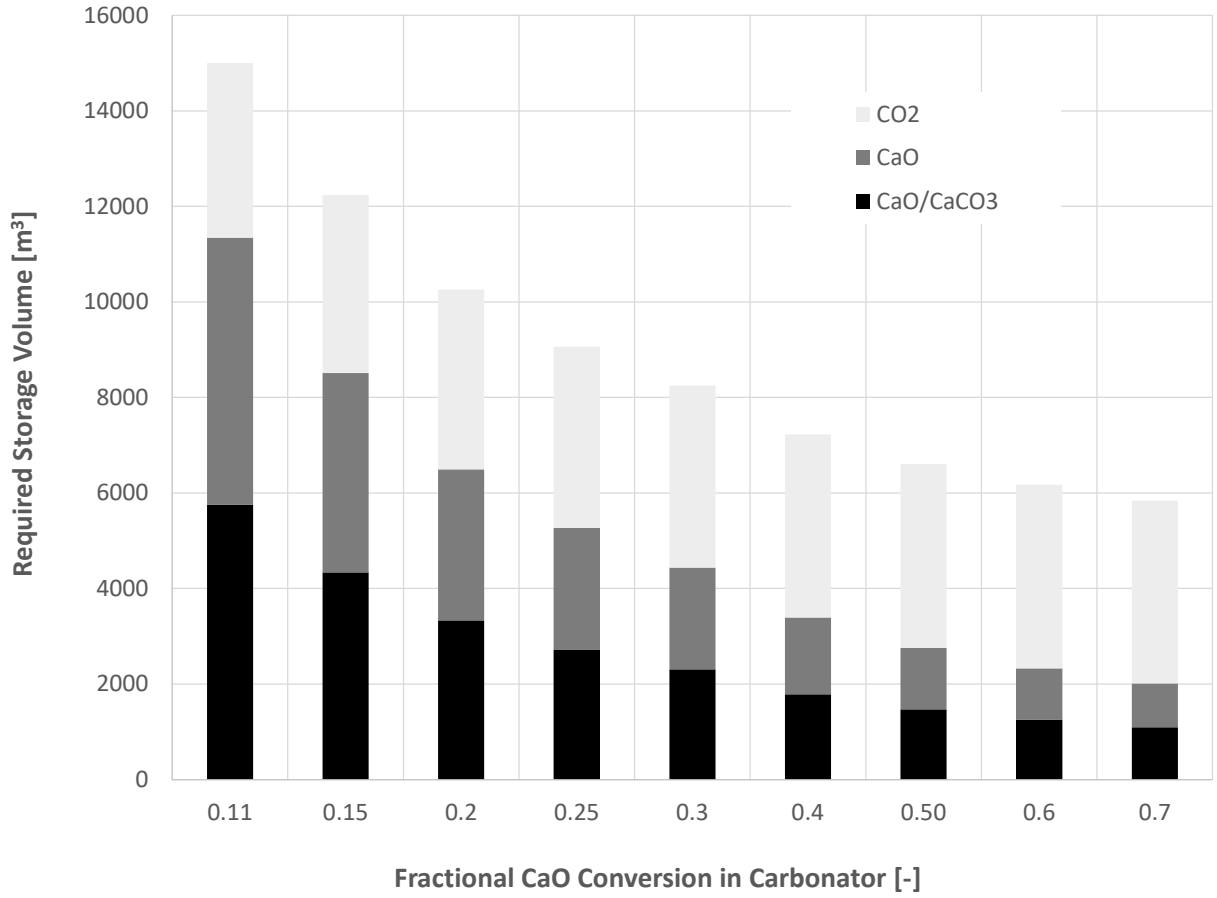

Figure 2-14: Required $CaO/CaCO_3$ storage volume as a function of fractional CaO conversion in the carbonator for Configuration 2

2.4.3. Comparison between Configuration 1 and Configuration 2

Figure 2-15 compares the storage cycle efficiency attained in Configuration 1 vs Configuration 2 as a function of fractional CaO conversion in the carbonator.

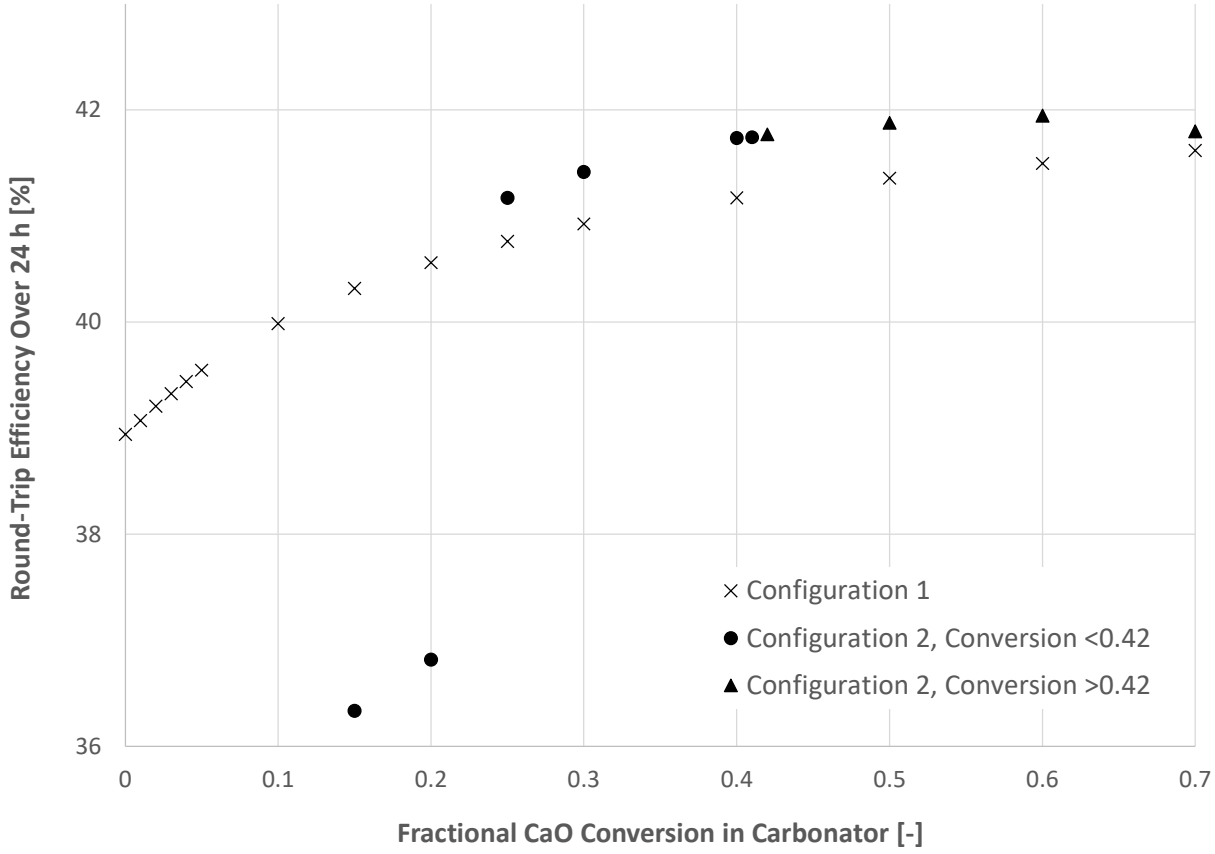

Figure 2-15: Storage cycle efficiency as a function of fractional CaO conversion in the carbonator, Configuration 1 vs Configuration 2

As previously noted, for Configuration 2, the heat balance on the carbonator side cannot be satisfied if the carbonation conversion is below 0.11. Again, the results are discontinuous at a carbonation conversion of 0.23 due to the switch from a subcritical to a supercritical steam cycle, and at a conversion of 0.41 due to the addition of HX-Q.

As shown, at low conversions, the round-trip efficiency is higher for Configuration 1. However, once the conversion exceeds 0.23 and the temperature of Stream 401 is sufficiently high to drive a supercritical steam cycle, the round-trip efficiency is higher for Configuration 2.

Figure 2-16 compares the required storage volume in Configuration 1 vs Configuration 2 as a function of fractional CaO conversion in the carbonator.

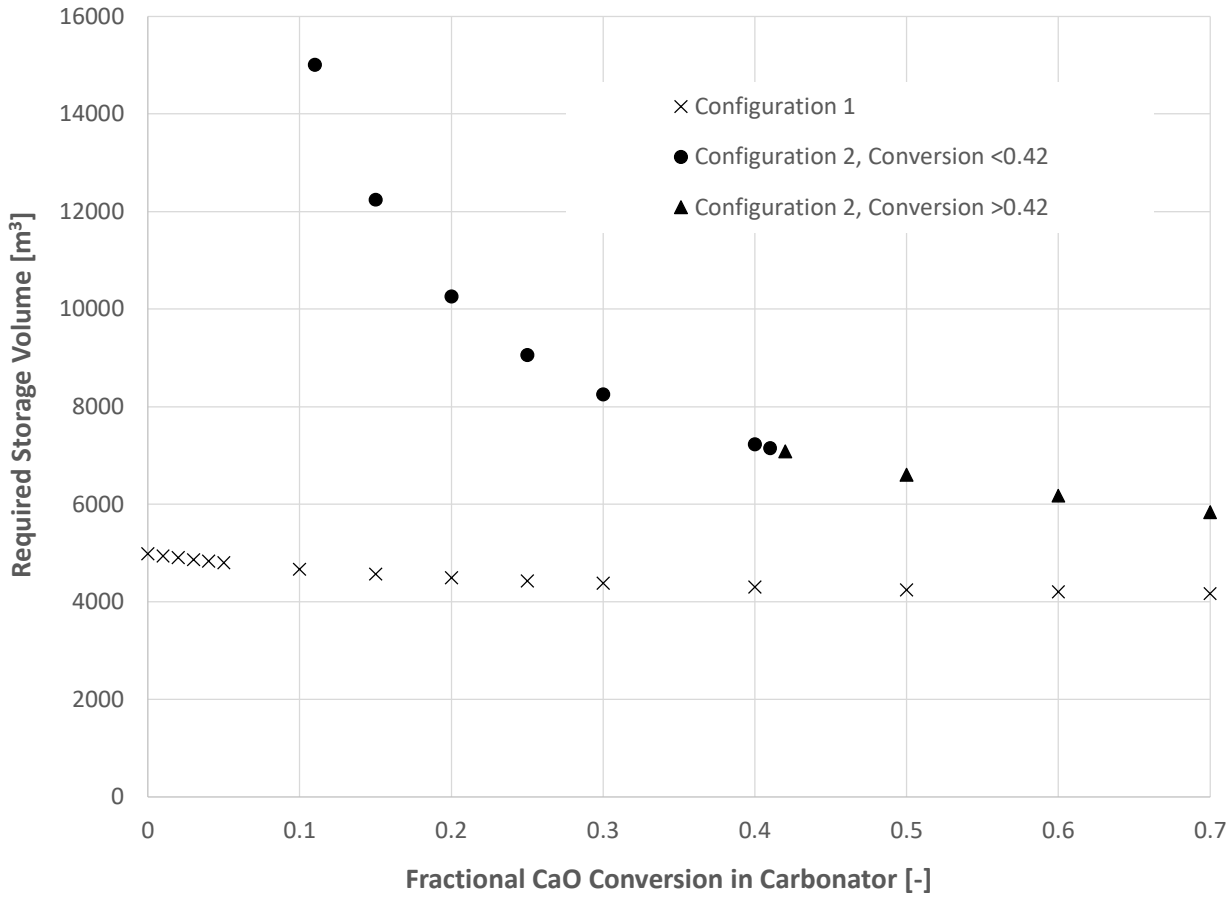

Figure 2-16: Required $CaO/CaCO_3$ storage volume as a function of fractional CaO conversion in the carbonator, Configuration 1 vs. Configuration 2

As shown, required storage volume is lower for Configuration 1, as well as a weaker function of conversion.

The energy storage density of the system can be estimated from the combined volume of the $CaO/CaCO_3$ storage vessel, the CaO storage vessel, and the sCO_2 storage vessel. Literature reports storage densities based on reaction enthalpies in the range of 2.5-3.2 GJ/m3 [23] [53], while other sources report lower values when taking into consideration the need for separate storage vessels and the conversion in the carbonator [54]. A recent analysis on storage density for CSP-CaL systems found energy density of the system ranged from 0.27 and 0.77 GJ/m^3 for carbonation conversion between 0.1 and 0.4 and with CO_2 storage at 75 bar [44]. The storage density was found to be mainly dependent on the CO_2 storage conditions (temperature and pressure) and the carbonation conversion.

Figure 2-17 presents the energy storage density as a function of carbonation conversion for both Configuration 1 and Configuration 2. Results are comparable to those obtained by Ortiz et al [44], with storage density ranging from 0.8-1.0 GJ/m^3 for Configuration 1 and 0.3-0.7 GJ/m^3 for Configuration 2.

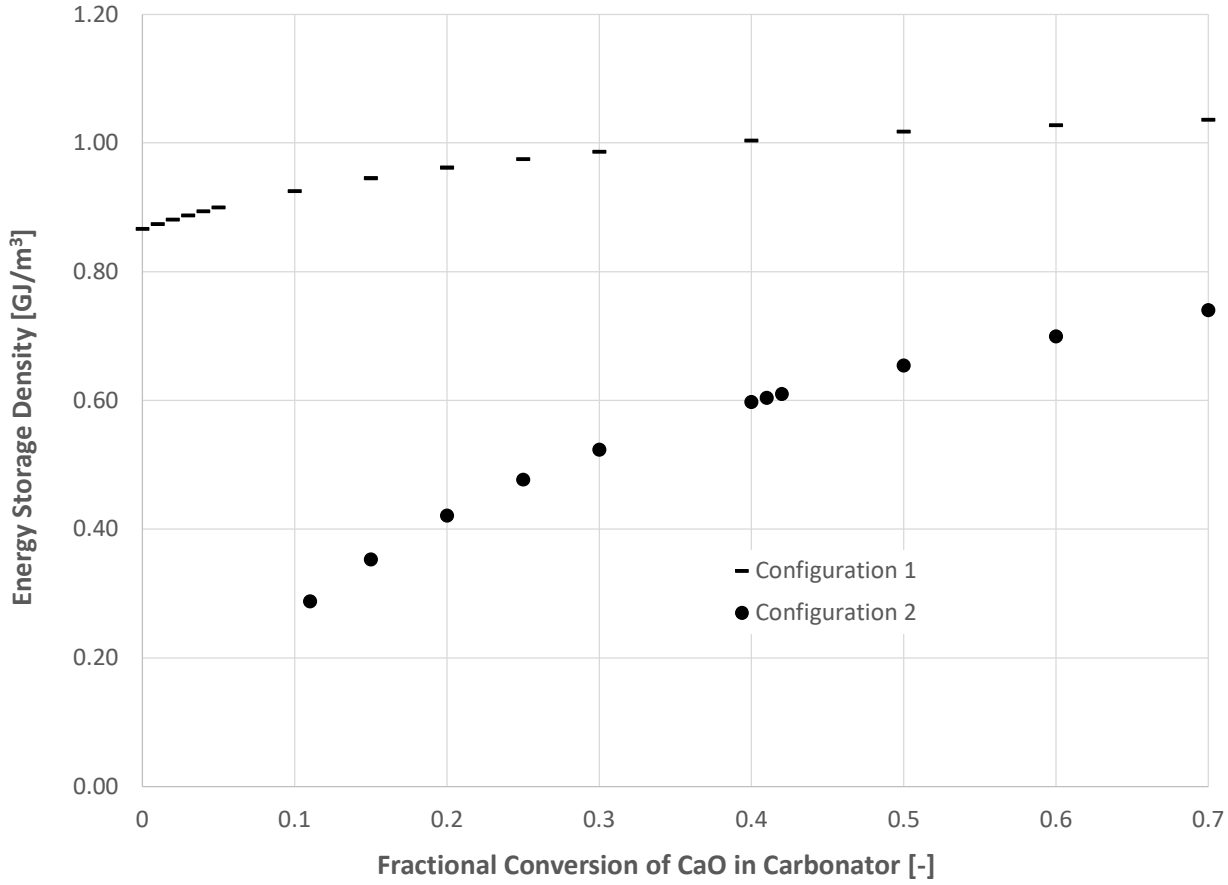

Figure 2-17: Energy storage density as a function of fractional CaO conversion in the carbonator

Figure 2-18 presents operating limits for both Configuration 1 and Configuration 2 as a function of carbonator solids inlet temperature at different values of fractional CaO conversion.

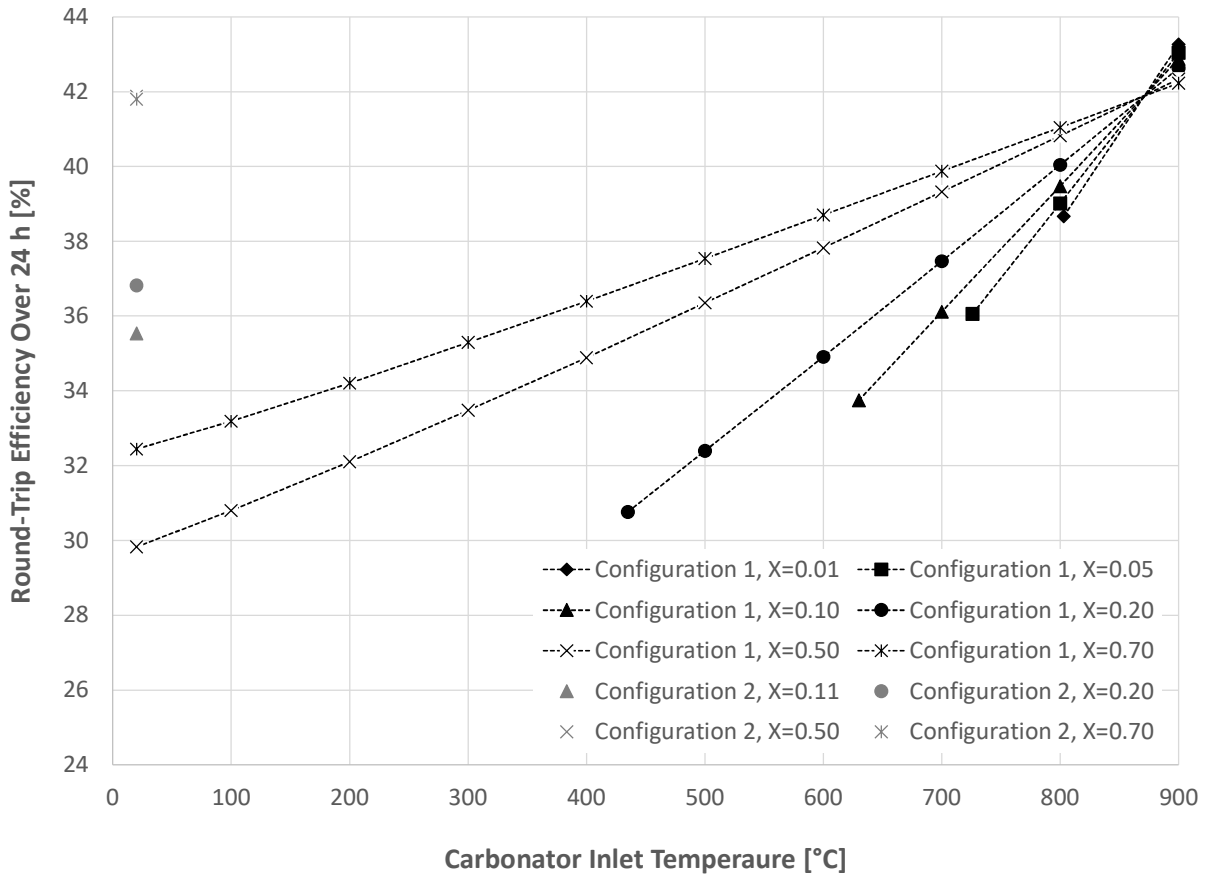

Figure 2-18: Operating limits for CaO conversion and carbonator solids inlet temperature

For Configuration 1, when a storage period of 12 hours is assumed, the carbonator solids inlet temperature (Stream 301) is determined by the rate of heat loss from the CaO storage vessel. As shown, the storage cycle efficiency increases rapidly with increasing carbonator inlet temperature, and the relationship is more pronounced at lower CaO conversions. However, lowering the CaO conversion introduces an operating limit on the carbonator inlet temperature – for example, at a conversion of 0.2, Stream 301 must enter the carbonator at a minimum temperature of 435°C in order for the heat balance to be satisfied; dropping the conversion to 0.05 increases this minimum temperature requirement to 726°C.

As noted previously, for Configuration 2, the heat balance requires a minimum conversion of 0.11. Above this minimum conversion, Configuration 2 will outperform Configuration 1 at lower carbonator inlet temperatures – for example, at a conversion of 0.2, a higher round-trip efficiency will be attained with Configuration 2 if a carbonator inlet temperature higher than approximately 680°C can't be attained with Configuration 1.

As Figure 2-18 shows, the selection between Configuration 1 and Configuration 2 will depend on the residual conversion of the solid material being used as well as the expected heat loss during the storage period.

Residual carbonation conversion of CaO

As noted in Section 2.1, the residual carbonation conversion of limestone has been studied extensively for applications in both CO_2 capture from combustion facilities and energy storage in CSP facilities. Much of the work conducted has been done via TGA. Studies indicate that although CaO carbonation conversion drops rapidly under CO_2 capture conditions for combustion applications, higher values of residual conversion may be attained under energy storage conditions [55]. However, the conditions considered for energy storage often include calcination under gas mixtures including helium or steam, allowing for lower calcination temperatures due to the lower partial pressure of CO_2 in the gas mixture. These calcination conditions are not reflected in many of the process analyses conducted [42] [56], which instead employ a 100% CO_2 atmosphere at 900°C. Under these conditions, sorbent deactivation can be expected to be similar to that observed in CO_2 capture processes. The residual carbonation conversion will also typically be lower in full-scale operation than in TGA testing, due to the impacts of sintering from operating the calciner as a fluidized bed. For example, pilot testing conducted over a 4-hour period in a 100 kW_{th} calciner at 910°C and under a 75% CO_2 / 5% N_2 / 20% O_2 atmosphere yielded a residual carbonation conversion of 0.07 [57]. Pilot testing conducted at the 1 MW_{th} scale over several days, in which the calciner was operated as an oxy-fired combustor with recirculated flue gas, yielded a residual carbonation conversion below 0.05 [58].

To attain the residual carbonation conversion required to operate in Configuration 2 (0.11), a number of options exist:

1. Implement a sorbent purge and make-up with fresh sorbent. This would lead to increased process complexity as well as increased operating costs in order to provide a supply of fresh sorbent.
2. Use a modified sorbent. Many techniques have been developed to improve the thermal and mechanical stability of calcium-based sorbents, including the use of rigid porous carrier materials, additives, and the use of synthetic precursors. Recent work has shown that acicular calcium and magnesium acetate precursor can yield a stable porous structure on the surface of calcium-based sorbents to permit an effective stable carbonation conversion up to 0.7 [52].
3. Employ enhanced calcination conditions, such as a partial steam or helium (He) environment, in order to reduce the CO_2 partial pressure and thereby reduce the operating temperature required to satisfy the equilibrium and achieve suitably fast calcination. This would require separation of the gas mixture downstream of the calciner before the CO_2 could be sent to storage; either via membrane for a He/CO_2 separation or via condensation for a steam/CO_2 separation. In addition to the required changes to the process configuration, this would have a significant impact on the calciner-side energy balance.

Heat loss from storage vessel

As shown in Figure 2-18, the benefit to round-trip efficiency of Configuration 1 vs Configuration 2 at lower values of carbonation conversion depends upon the temperature of the solids entering the carbonator (Stream 301). For Configuration 1, this is dictated by the quantity of heat lost in the CaO storage vessel. Heat loss from the storage vessel will depend upon two parameters, namely

- The rate of heat loss from the vessel to the atmosphere, and
- The storage duration, i.e. the length of time the CaO is stored for.

In the base case modelled for this work, the storage duration is 12 h. However, one of the noted benefits of thermochemical energy storage is its potential for theoretically unlimited storage durations, due to the fact that the products of calcination are stable and can be stored at ambient temperature without deteriorating. For this reason, the process may be considered as a solution in circumstances where longer-term energy storage, e.g. seasonal storage, is required.

The rate of heat loss from the vessel to the atmosphere can be estimated through a simple heat transfer analysis. This was done based on the assumption that the greatest resistance to heat transfer from the storage vessel will be at the surface, where heat loss will occur via free convection and radiation. This analysis represents a worst-case scenario where resistance to conductive heat loss through the vessel is neglected, and the vessel surface is assumed to be at the same temperature as the stored solids. The vessel is assumed to be a vertical cylinder with an L/D ratio of 3.

The rate of heat loss from the CaO storage vessel is estimated as the sum of convective and radiative heat loss according to Equation 2-10 [59].

$$Q = [\overline{h}\pi D(T_s - T_\infty) + \varepsilon\pi D\sigma(T_s^4 - T_\infty^4)]L \qquad \text{Equation 2-10}$$

Here, Q is the overall rate of heat loss [W]; h is the average convection coefficient [W/m^2K]; D is the diameter of the storage vessel [m]; T_s is the surface temperature of the vessel [°C]; T_∞ is the temperature of the surroundings [°C], ε is the emissivity of the surface [-], σ is the Stefan Boltzmann constant [$5.67x10^{-8}$ W/m^2K^4]; and L is the length of the storage vessel.

The quantity of solids in the storage tank was calculated based on operation of the calciner for 12 hours. A heat loss rate, in °C/h, was then calculated by rearranging Equation 2-11 for ΔT/t.

$$Q = mC_p\frac{\Delta T}{t} \qquad \text{Equation 2-11}$$

Here, Q is the rate of heat loss calculated using Equation 2-10 [W]; C_p is the heat capacity of CaO [kJ/kg°C]; ΔT is the change in the temperature of the solids [°C], and t is the time over which that temperature change occurred [h].

Results indicate that, for a carbonation conversion of 0.2, the heat loss rate starts at approximately 1.8°C/h and decreases as the surface temperature of the vessel decreases. For a carbonation conversion of 0.05, the heat loss rate starts slightly lower, at 1.6°C/h, due to the larger thermal mass of solids in the system. The carbonator solids inlet temperature is assumed to be the same as the CaO storage tank temperature. Figure 2-19 shows the carbonator solids inlet temperature as a function of storage duration for Configuration 1. Results are shown for both the base case ambient temperature (T_∞ in Equation 2-10) of 20°C and an ambient temperature of -20°C.

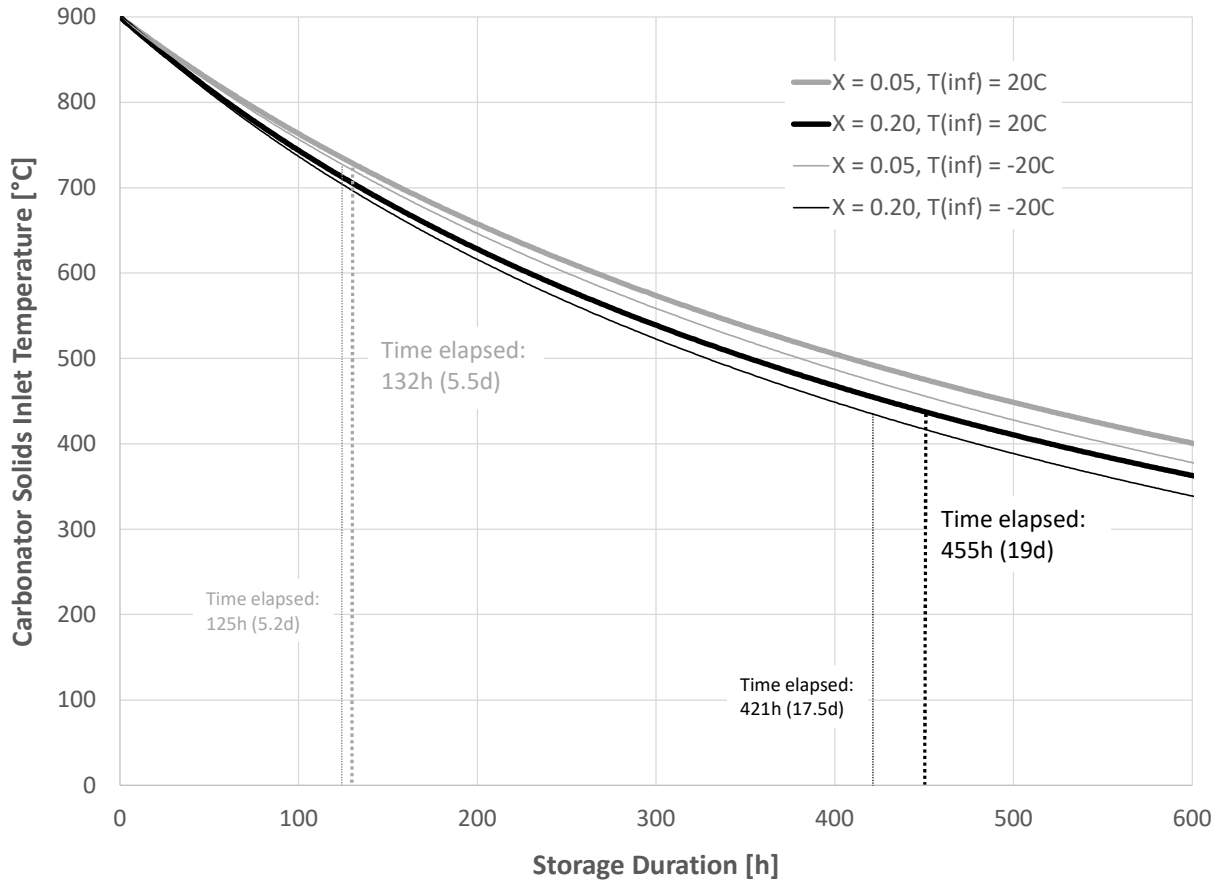

Figure 2-19: Carbonator solids inlet temperature as a function of storage duration for Configuration 1

As shown, for a carbonation conversion of 0.2 and ambient temperature of 20°C, the carbonator solids inlet temperature reaches the limit of 435°C dictated by Figure 2-18 after 455 h, or approximately 19 days. This limit is reached within 17.5 days if the ambient temperature is -20°C. For a carbonation conversion of 0.05 and ambient temperature of 20°C, the carbonator solids inlet temperature reaches the limit of 726°C within 132 h, or 5.5 days. In this case, the limit is reached within 5.2 days if the ambient temperature is -20°C.

If a longer storage duration were required in configuration 1, such as in the case of seasonal storage, it would still be possible to use the proposed carbonate system, as the calcination products are stable at ambient temperature. However, it would be necessary to add additional process equipment, including auxiliary heating on the carbonator side for process start-up, which would add a significant efficiency penalty and make the system less competitive with other storage technologies. To determine the efficiency and overall competitiveness of the proposed system under long-term storage conditions, a transient analysis would be required to evaluate start-up energy requirements.

Overall process complexity

Further to considerations on the overall process efficiency, the process complexity, as dictated by the required process equipment and conditions, should be taken into account when comparing Configuration 1 to Configuration 2. As shown in Figure 2-5, Figure 2-6, and Figure 2-7, Configuration 2 introduces two additional heat exchangers, including a solid-solid heat exchanger on the calciner side. Further, the larger quantity of solids circulating in the system in Configuration 2 leads to an increase in size for all vessels, as well as increased conveying duty. Although costs have not been assessed as part of this study, it is reasonable to assume that both capital and operating costs would be higher for Configuration 2 as a result of these factors.

2.4.4. Comparison of proposed system to other proposed CSP-CaL systems

The technical merits of the proposed system, relative to other proposed CSP-CaL systems, can be assessed in terms of overall process efficiency, energy storage density, and process complexity.

Round-trip storage cycle efficiency

As noted in Section 2.1, previous research has reported round-trip storage cycle efficiencies in the range of 38-46% as a function of carbonation conversion. As shown in Figure 2-8, for Configuration 1, comparable efficiencies are achievable with the proposed configuration at supercritical steam cycle efficiencies over about 39%. For Configuration 2, as shown in Figure 2-13, round-trip efficiency is somewhat lower, reaching a maximum of 42% for the supercritical steam cycle efficiency selected.

Energy storage density

As shown in Figure 2-17, for Configuration 1, the energy storage density is between 0.8 and 1.0 GJ/m^3 for carbonation conversions between 0 and 0.7. For Configuration 2, the storage density is between 0.3 and 0.7 for carbonation conversions between 0.11 and 0.7. This is comparable to values obtained by Ortiz et al [44], who reported energy densities in the range of 0.27 to 0.77 GJ/m^3 for carbonation conversions of 0.1 to 0.4.

Process complexity

An important difference in the proposed system relative to other proposed CSP-CaL processes is that the calciner, the carbonator, and the solids storage vessels are all operated at atmospheric pressure, eliminating the requirement for lockhoppering of solids, which can introduce significant process complexity, especially if high-temperature lock hoppers are required.

Further, the separation between the main turbine working fluid and the carbonator enables decoupling of the turbine pressure and the carbonator pressure. This allows for a multi-stage turbine with a pressure ratio that can be selected independently of the carbonator operating pressure, and eliminates the necessity presented in some configurations of operating the turbine outlet under vacuum. To fully assess the benefits of operating the turbine in this configuration, including the potential to implement interstage

reheating and increase overall efficiency, a more sophisticated analysis of the power cycle would be required.

On the other hand, with the proposed system, a significant amount of energy on the carbonator side is attained from either a supercritical steam cycle, a subcritical steam cycle, or a combination of both. This requires additional equipment and adds complexity relative to other CSP-CaL processes. As noted, further assessment of the sCO_2 power cycle could increase energy produced in the main turbine, and decrease or eliminate the requirement for a steam cycle.

2.5. Bringing the CSP-CaL process to market

As demonstrated by the extensive work conducted on the integration of CSP with the CaL process for energy storage, there is significant interest in the technology and vision for its competitive success in the energy market. However, a number of challenges remain to be addressed before CSP-CaL can be successfully deployed, including

- Techo-economic challenges, including design of major process components such as the solar calciner, limitations of the multicycle residual conversion of CaO, and solids handling requirements;
- Demonstration of tangible environmental benefits associated to displacing conventional thermal power generation with CSP-CaL; and
- Generation of social, political, and policy support for the concept.

2.5.1. Techno-economic challenges

To address the technical barriers remaining for CSP-CaL, a number of projects have been conducted in recent years, including laboratory-scale work, simulation-based process modelling, and, more recently, pilot-scale research.

The SOCRATCES project is a planned pilot aimed at demonstrating the feasibility of the CSP-CaL integration and reducing the core risks associated with scaling up the technology. The project team includes the University of Seville, as well as a number of other European universities and technology developers, and is funded by the European Commission's Horizon 2020 Programme for Research and Innovation. The expected results of the project include testing the system at TRL 5; demonstrating flash calcination technology at prototype scale; carbonator design with the possibility for scale-up and integration with a power block; analysis of attrition, agglomeration, and fouling; successful control of solids handling; and assessment of precursor materials and process conditions to allow high residual sorbent activity [60].

Supported by the ELEMENTS program under the US DOE SunShot Initiative, a project titled "Regenerative Carbonate-Based Thermochemical Energy Storage System for Concentrating Solar Power" was conducted in 2015-2016 to overcome the limitations of residual CaO conversion. The researchers developed a synthetic reinforced CaO sorbent with a residual sorbent capacity around 0.3; however, fabrication of this material would significantly increase both cost and technical complexity of the CaL process [47].

A follow-on to this project titled "Demonstration of High-Temperature Calcium-Based Thermochemical Storage System for use with Concentrating Solar Power Facilities" was funded by the US DOE's APOLLO program and conducted between 2015 and 2018. The project focused on optimization and scale-up of the system, including validating the CaO sorbent for capacity, durability, and system economics. The researchers designed, fabricated, and commissioned a 4 kW_{th} pilot facility that included a closed-loop CO_2 system and a packed bed heat exchanger reactor. They were able to demonstrate operation of this system through short charging and discharging periods. They also conducted a techno-economic analysis (TEA) to estimate cost per kWh_{th} of energy stored, and translated this to an LCOE [61]. In 2019, they attained a patent for the system [62].

2.5.2. Environmental Impact

The ultimate goal of the CSP-CaL process is to reduce GHG emissions by displacing conventional thermal power generation. In order to determine if it will, in fact, accomplish this, it is necessary to fully evaluate the impact of displacing once process with another. A popular tool for conducting this type of evaluation is Life Cycle Assessment, which can assess the impacts of products and systems from the cradle to the grave [63]. It involves quantifying inputs to and outputs from a product or system over its full life cycle, and assigning impacts to those inputs and outputs. These impacts can include costs, energy requirements, and environmental performance indicators. Evaluation of these impacts can be used to identify stages in a process which contribute significantly to a certain impact, as well as to compare the overall impact of a given product or system to another. Although a full LCA is outside the scope of this work, the requirements for conducting an LCA are considered here to inform future work.

Conducting an LCA to evaluate environmental performance begins with definition of the goal and scope of the assessment. This includes

- A goal statement. In the case of the proposed CSP-CaL system, this could be determining the full life cycle impact of the system in order to compare these impacts with conventional power generation systems, compare with other renewable energy/energy storage combinations, and/or identify points in the life cycle where impacts can be reduced;
- Determining the impacts to be considered, such as GHG emissions, other pollutant emissions, and land usage;
- Determining the functional unit that will serve as the basis for evaluating these impacts. For a power generation process, the functional unit would typically be kW/MW or kWh/MWh exiting the process. This enables normalization of the results of the LCA in a manner that lends itself easily to comparison – for example, GHG emissions can be reported as $kgCO_{2eq}$/MWh; and
- Defining the spatial and temporal boundaries of the system that will be considered to fall within the life cycle. This is what sets LCA apart from other types of environmental assessment; it allows for evaluation of impacts during extraction of primary resources, manufacture of equipment, and disposal at the end of the system lifetime.

Once the goal and scope have been defined, the next step is inventory analysis. This involves development of a block flow diagram for the full life cycle of the process, based on the boundaries identified in the

previous step. An example of what this could look like for a CSP-CaL process is shown in Figure 2-20, with blocks representing sub-processes and arrows representing material and energy flows. In this example, the impact of interest is GHG emissions, shown in $kgCO_{2eq}$/h. Depending on the goal statement, the boundaries of the LCA could be adjusted to include or exclude processes as appropriate. Material and energy flows would be quantified from a combination of process simulation results, LCA database information, and other publicly available process information.

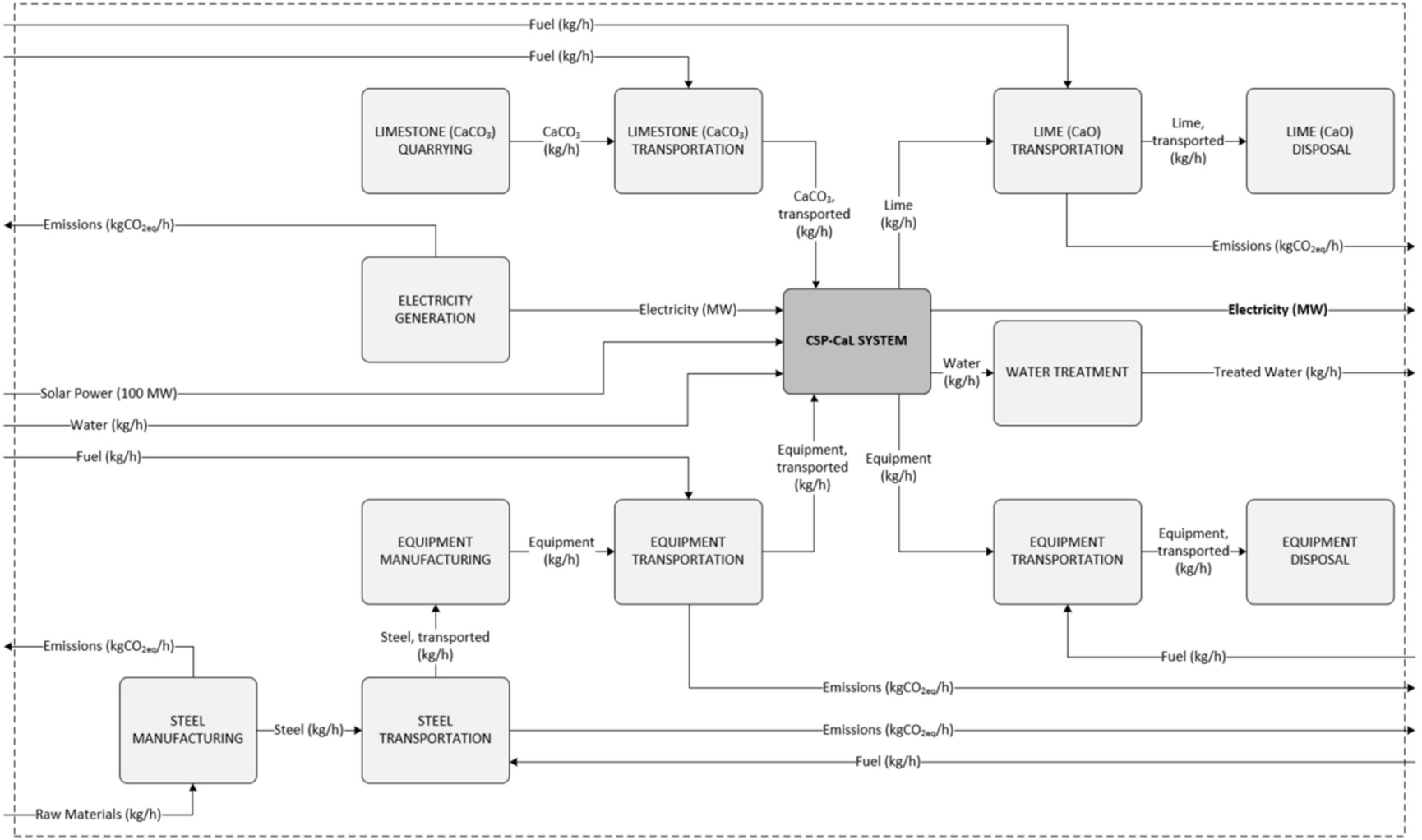

Figure 2-20: Block flow diagram for life cycle assessment of CSP-CaL process

With the inventory analysis complete, an impact assessment can be conducted. This part of the LCA takes the results of the inventory analysis and translates them into relevant information describing the impact on receptors, such as human populations and ecosystems.

With the comprehensive view of the environmental impacts that a CSP-CaL system would have over its lifetime, it would be possible to compare these impacts with other systems for which similar analyses have been conducted. Comparable systems could include conventional fossil fuel power generation, such as a natural gas plant; a nuclear power facility; or a given regional grid mix combined with another energy storage technology (e.g. CAES, pumped hydro, or battery). While one system might, for example, lead to more GHG emissions over its lifetime, it might also require more primary resource or land usage, or result in higher emissions of other pollutants. The results of the LCA could also be used to identify what stages in the life cycle of a CSP-CaL contribute the most to different impacts, and provide opportunities to focus development on reducing impacts at these stages.

2.5.3. Sociopolitical support

The proposed energy storage system may face challenges in obtaining sociopolitical support on two fronts: first, the nature and implications of energy storage itself; and second, the fact that it involves storage of compressed CO_2.

Although energy storage technologies can offer benefits to conventional fossil fuel generation, their true value lies in their potential role in supporting the transition to future low-carbon energy systems [64]. These systems are socio-technological systems that involve not only equipment and resources, but also energy technology designers, managers, and consumers. As such, efforts to change these systems involve change to the complex social and economic assemblages that are built around them. Energy policy to guide these changes will need to be critically reflective of the social dimensions surrounding energy systems [65]. These dimensions stem from interactions among three system “levels”: niche innovations, regimes (i.e. the status quo), and landscape (long-term trends). System transitions involve a shift from one regime configuration to another, which can result in the displacement of previously dominant actors or technologies [64].

In Canada, Ontario and Alberta are the most active regions in development of energy storage. However, even in these regions, and in Canada as a whole, technical advancements in the technology are outpacing the socio-political conditions, such as regulations and public awareness, that would be required to support deployment of these technologies [13][66]. A lack of coordination among stakeholders, including regulators, power producers, and policymakers, plays a significant role in the absence of these conditions [67]. Recent research into media representation of energy storage in Canada has shown a link between changes in energy policy and public interest in energy storage technologies. This is both promising and challenging, as it implies that while public awareness may be required to support development of necessary regulations, the development of such regulations may also be an important driver for public awareness. Further, although analysis of media representation of energy storage in Ontario and Alberta between 2007 and 2017 showed an overall optimistic perspective, it is still perceived as somewhat risky and uncertain, more notably in Alberta where the economy traditionally relies heavily on the fossil fuel

industry [66]. This shines light on the important issue of energy justice, which considers who benefits and who is put at risk by energy transitions. Often, the distribution of impacts from energy production and use are highly unequal, as are the consequent economic and political benefits [65].

Beyond the concerns and implications associated to the role of energy storage in transitioning to a low-carbon economy, and perhaps more significant to the proposed CSP-CaL process, is the public opinion of CO_2 utilization and storage. Depending on the scale at which a storage system involving the CaL process is implemented, storage of large volumes of CO_2 could be required, and in some cases geological storage might be suitable. As such, the proposed storage system may be subject to the same criticisms that are levelled at carbon capture and storage (CCS) technology.

Leiss and Larkin (2019) identify public acceptability as one of the key social dimensions that will influence the feasibility of CCS [68]. Acceptability begins with awareness, and research has shown that public awareness of CCS as an energy technology, both globally and within Canada, ranges from low to moderate, with a 2011 survey reporting only 14% of Canadians knew what CCS was [69], [70]. On a more positive note, a 2013 study in which participants in a workshop on CCS were surveyed on their attitudes towards CCS before and after the workshop showed that Canadian respondents significantly increased their support for CCS after participating [70]. However, other research shows that the strongest predictors of acceptance of CCS are its perceived benefits along with the perceived risk, such as leakage and environmental impacts [71].

3. Conclusions and Recommendations

The configuration of the CSP-CaL process proposed in this work offers some advantages to other proposed configurations. In particular, operating both the calciner and the carbonator at atmospheric pressure eliminates the need for lock hoppering of hot solids, which reduces the process complexity. Configuration 1 further offers the elimination of solid-solid heat exchangers, which are not a commercially developed technology. The results obtained through process simulation indicate that the proposed process is capable of achieving round trip efficiencies in the range of 32-46% and energy storage densities in the range of 0.3-1.0 GJ/m^3. These parameters are strongly dependent on the residual conversion of the CaO sorbent as well as the efficiency of the power cycles used to remove heat on the carbonator side of the process.

In order to bring the CSP-CaL process to market, a number of technical challenges must be overcome. The deactivation of calcium oxide over multiple cycles, leading to low residual conversion, means that large volumes of inactive sorbent will be circulating in the process. This requires larger equipment, increasing both capital and operating costs and decreasing the energy storage density. Further, as noted, the solid-solid heat exchangers required in Configuration 2 are not yet a commercial technology. Other technical issues, such as challenges associated to high-temperature solids handling, may make it difficult for the CSP-CaL process to compete with other less-complex energy storage technologies. Additionally, solar particle receivers are not sufficiently developed to bring the technology to market; however, as noted, the proposed CaL process is not dependent on the source of heat input and could also be used to store electricity from the grid via electric heating.

The proposed process may also face barriers in gaining sociopolitical support. Energy storage technologies play a significant role in the transition to a low-carbon future and may face resistance from actors that benefit from the continued success of the fossil fuel industry. Further, the lack of public awareness and acceptance for CO_2 storage and utilization technologies may hinder large-scale deployment of the process.

In order to more fully understand the potential for this combined compressed gas and thermochemical energy storage process to compete with other energy storage technologies on the market, a more thorough environmental assessment should be conducted, with life cycle assessment being the recommended tool. The process is designed to release zero CO_2 to the atmosphere, which initially makes it appear to be preferable to traditional CAES from a climate change perspective. Further, the increased storage density associated with the thermochemical process, in comparison with a strictly thermal process, makes it competitive with AA-CAES from an efficiency standpoint. However, analysis is required to determine if the full life cycle of the process can in fact lead to an overall decrease in GHG emissions relative to these other technologies.

References

[1] J. D. S. CNN Joshua Berlinger and Ralph Ellis, "COP21: Obama praises Paris climate change agreement," *CNN*, Dec. 14, 2015. https://www.cnn.com/2015/12/12/world/global-climate-change-conference-vote/index.html (accessed Jul. 24, 2020).

[2] T. A. P. · P. Dec 05, 2018 5:47 PM ET | Last Updated: December 5, and 2018, "Global carbon dioxide emissions rose almost 3% in 2018 | CBC News," *CBC*, Dec. 05, 2018. https://www.cbc.ca/news/technology/carbon-pollution-increase-1.4934096 (accessed Jul. 24, 2020).

[3] S. Pacala, "Stabilization Wedges: Solving the Climate Problem for the Next 50 Years with Current Technologies," *Science*, vol. 305, no. 5686, pp. 968–972, Aug. 2004, doi: 10.1126/science.1100103.

[4] S. J. Davis, L. Cao, K. Caldeira, and M. I. Hoffert, "Rethinking wedges," *Environ. Res. Lett.*, vol. 8, no. 1, p. 011001, Mar. 2013, doi: 10.1088/1748-9326/8/1/011001.

[5] P. Charriau and M. Crenes, "A step backward for the energy transition?," p. 39.

[6] Environment and Climate Change Canada, "Greenhouse gas emissions," *aem*, Apr. 15, 2020. https://www.canada.ca/en/environment-climate-change/services/environmental-indicators/greenhouse-gas-emissions.html (accessed Jul. 24, 2020).

[7] Environment and Climate Change Canada Government of Canada, "Canada's mid-century long-term low-greenhouse gas development strategy," Government of Canada, Gatineau, Canada, 978-0-660-06577–9, 2016.

[8] "Acting on Climate Change: Solutions from Canadian Scholars." Sustainable Canada Dialogues, Mar. 2015. [Online]. Available: http://www.sustainablecanadadialogues.ca/en/scd/endorsement

[9] "National Energy Board 2016 - Canada's Renewable Power Landscape.pdf."

[10] P. Denholm and T. Mai, "Timescales of Energy Storage Needed for Reducing Renewable Energy Curtailment," *Renew. Energy*, p. 33, 2017.

[11] "Unleashing-the-Value-of-Energy-Storage-Dr-Andrew-Ford-NRStor.pdf."

[12] N. Günter and A. Marinopoulos, "Energy storage for grid services and applications: Classification, market review, metrics, and methodology for evaluation of deployment cases," *J. Energy Storage*, vol. 8, pp. 226–234, Nov. 2016, doi: 10.1016/j.est.2016.08.011.

[13] S. Ganowski and I. H. Rowlands, "Read all about it! Comparing media discourse on energy storage in Canada and the United Kingdom in a transition era," *Energy Res. Soc. Sci.*, vol. 70, p. 101709, Dec. 2020, doi: 10.1016/j.erss.2020.101709.

[14] "Technology Roadmap Energy storage," p. 64, 2014.

[15] M. Budt, D. Wolf, R. Span, and J. Yan, "A review on compressed air energy storage: Basic principles, past milestones and recent developments," *Appl. Energy*, vol. 170, pp. 250–268, May 2016, doi: 10.1016/j.apenergy.2016.02.108.

[16] J. Konrad, R. Carriveau, M. Davison, F. Simpson, and D. S.-K. Ting, "Geological compressed air energy storage as an enabling technology for renewable energy in Ontario, Canada," *Int. J. Environ. Stud.*, vol. 69, no. 2, pp. 350–359, Apr. 2012, doi: 10.1080/00207233.2012.663228.

[17] X. Luo, J. Wang, M. Dooner, J. Clarke, and C. Krupke, "Overview of Current Development in Compressed Air Energy Storage Technology," *Energy Procedia*, vol. 62, pp. 603–611, 2014, doi: 10.1016/j.egypro.2014.12.423.

[18] "BINE Informationsdienst - Compressed air energy storage power plants.pdf."

[19] "Brochure-ADELE.pdf."

[20] "Projects – Hydrostor." https://www.hydrostor.ca/projects/ (accessed Aug. 13, 2020).

[21] "SAS-AGM-Keynote-Presentation.pdf."

[22] A. H. Abedin and M. A. Rosen, "A critical review of thermochemical energy storage systems," *Open Renew. Energy J*, vol. 4, pp. 42–46, 2011.
[23] P. Pardo, A. Deydier, Z. Anxionnaz-Minvielle, S. Rougé, M. Cabassud, and P. Cognet, "A review on high temperature thermochemical heat energy storage," *Renew. Sustain. Energy Rev.*, vol. 32, pp. 591–610, Apr. 2014, doi: 10.1016/j.rser.2013.12.014.
[24] H. Ibrahim, A. Ilinca, and J. Perron, "Energy storage systems—Characteristics and comparisons," *Renew. Sustain. Energy Rev.*, vol. 12, no. 5, pp. 1221–1250, Jun. 2008, doi: 10.1016/j.rser.2007.01.023.
[25] Richard Blackwell, "Temporal Power spinning renewable energy wheels," *The Globe and Mail*, Toronto, Canada, Nov. 10, 2014. Accessed: Aug. 14, 2020. [Online]. Available: https://www.theglobeandmail.com/report-on-business/industry-news/energy-and-resources/temporal-power-spinning-renewable-energy-wheels/article21526794/?ref=http://www.theglobeandmail.com&
[26] A. Castillo and D. F. Gayme, "Grid-scale energy storage applications in renewable energy integration: A survey," *Energy Convers. Manag.*, vol. 87, pp. 885–894, Nov. 2014, doi: 10.1016/j.enconman.2014.07.063.
[27] A. Abdon, X. Zhang, D. Parra, M. K. Patel, C. Bauer, and J. Worlitschek, "Techno-economic and environmental assessment of stationary electricity storage technologies for different time scales," *Energy*, vol. 139, pp. 1173–1187, Nov. 2017, doi: 10.1016/j.energy.2017.07.097.
[28] M. Aneke and M. Wang, "Energy storage technologies and real life applications – A state of the art review," *Appl. Energy*, vol. 179, pp. 350–377, Oct. 2016, doi: 10.1016/j.apenergy.2016.06.097.
[29] B. Zakeri and S. Syri, "Electrical energy storage systems: A comparative life cycle cost analysis," *Renew. Sustain. Energy Rev.*, vol. 42, pp. 569–596, Feb. 2015, doi: 10.1016/j.rser.2014.10.011.
[30] R. Symonds, "Development of a Continuous Calcium Looping Process for CO2 Capture," Thesis, Université d'Ottawa / University of Ottawa, 2017. doi: http://dx.doi.org/10.20381/ruor-20734.
[31] J. M. Valverde, P. E. Sanchez-Jimenez, and L. A. Perez-Maqueda, "Ca-looping for postcombustion CO2 capture: A comparative analysis on the performances of dolomite and limestone," *Appl. Energy*, vol. 138, pp. 202–215, Jan. 2015, doi: 10.1016/j.apenergy.2014.10.087.
[32] C. Ortiz, R. Chacartegui, J. M. Valverde, J. A. Becerra, and L. A. Perez-Maqueda, "A new model of the carbonator reactor in the calcium looping technology for post-combustion CO2 capture," *Fuel*, vol. 160, pp. 328–338, Nov. 2015, doi: 10.1016/j.fuel.2015.07.095.
[33] G. S. Grasa and J. C. Abanades, "CO_2 Capture Capacity of CaO in Long Series of Carbonation/Calcination Cycles," *Ind. Eng. Chem. Res.*, vol. 45, no. 26, pp. 8846–8851, Dec. 2006, doi: 10.1021/ie0606946.
[34] D. P. Hanak, A. J. Kolios, and V. Manovic, "Comparison of probabilistic performance of calcium looping and chemical solvent scrubbing retrofits for CO 2 capture from coal-fired power plant," *Appl. Energy*, vol. 172, pp. 323–336, Jun. 2016, doi: 10.1016/j.apenergy.2016.03.102.
[35] C. Tregambi, M. Troiano, F. Montagnaro, R. Solimene, and P. Salatino, "Fluidized Beds for Concentrated Solar Thermal Technologies—A Review," *Front. Energy Res.*, vol. 9, p. 618421, Apr. 2021, doi: 10.3389/fenrg.2021.618421.
[36] C. Ortiz, J. M. Valverde, R. Chacartegui, and L. A. Perez-Maqueda, "Carbonation of Limestone Derived CaO for Thermochemical Energy Storage: From Kinetics to Process Integration in Concentrating Solar Plants," *ACS Sustain. Chem. Eng.*, vol. 6, no. 5, pp. 6404–6417, May 2018, doi: 10.1021/acssuschemeng.8b00199.
[37] S. A. Salaudeen, B. Acharya, and A. Dutta, "CaO-based CO2 sorbents: A review on screening, enhancement, cyclic stability, regeneration and kinetics modelling," *J. CO2 Util.*, vol. 23, pp. 179–199, Jan. 2018, doi: 10.1016/j.jcou.2017.11.012.

[38] M. Benitez-Guerrero, J. M. Valverde, P. E. Sanchez-Jimenez, A. Perejon, and L. A. Perez-Maqueda, "Multicycle activity of natural CaCO 3 minerals for thermochemical energy storage in Concentrated Solar Power plants," *Sol. Energy*, vol. 153, pp. 188–199, Sep. 2017, doi: 10.1016/j.solener.2017.05.068.
[39] B. Sarrión, A. Perejón, P. E. Sánchez-Jiménez, L. A. Pérez-Maqueda, and J. M. Valverde, "Role of calcium looping conditions on the performance of natural and synthetic Ca-based materials for energy storage," *J. CO2 Util.*, vol. 28, pp. 374–384, Dec. 2018, doi: 10.1016/j.jcou.2018.10.018.
[40] S. E. B. Edwards and V. Materić, "Calcium looping in solar power generation plants," *Sol. Energy*, vol. 86, no. 9, pp. 2494–2503, Sep. 2012, doi: 10.1016/j.solener.2012.05.019.
[41] R. Chacartegui, A. Alovisio, C. Ortiz, J. M. Valverde, V. Verda, and J. A. Becerra, "Thermochemical energy storage of concentrated solar power by integration of the calcium looping process and a CO2 power cycle," *Appl. Energy*, vol. 173, pp. 589–605, Jul. 2016, doi: 10.1016/j.apenergy.2016.04.053.
[42] A. Alovisio, R. Chacartegui, C. Ortiz, J. M. Valverde, and V. Verda, "Optimizing the CSP-Calcium Looping integration for Thermochemical Energy Storage," *Energy Convers. Manag.*, vol. 136, pp. 85–98, Mar. 2017, doi: 10.1016/j.enconman.2016.12.093.
[43] C. Ortiz, R. Chacartegui, J. M. Valverde, A. Alovisio, and J. A. Becerra, "Power cycles integration in concentrated solar power plants with energy storage based on calcium looping," *Energy Convers. Manag.*, vol. 149, pp. 815–829, Oct. 2017, doi: 10.1016/j.enconman.2017.03.029.
[44] C. Ortiz, M. C. Romano, J. M. Valverde, M. Binotti, and R. Chacartegui, "Process integration of Calcium-Looping thermochemical energy storage system in concentrating solar power plants," *Energy*, vol. 155, pp. 535–551, Jul. 2018, doi: 10.1016/j.energy.2018.04.180.
[45] C. Ortiz, R. Chacartegui, J. M. Valverde, A. Carro, C. Tejada, and J. Valverde, "Increasing the solar share in combined cycles through thermochemical energy storage," *Energy Convers. Manag.*, vol. 229, p. 113730, Feb. 2021, doi: 10.1016/j.enconman.2020.113730.
[46] D. P. Hanak, C. Biliyok, and V. Manovic, "Calcium looping with inherent energy storage for decarbonisation of coal-fired power plant," *Energy Environ. Sci.*, vol. 9, no. 3, pp. 971–983, 2016, doi: 10.1039/C5EE02950C.
[47] C. Ortiz, J. M. Valverde, R. Chacartegui, L. A. Pérez-Maqueda, and P. Gimenez-Gavarrell, "Scaling-up the Calcium-Looping Process for CO_2 Capture and Energy Storage," *KONA Powder Part. J.*, vol. 38, no. 0, pp. 189–208, Jan. 2021, doi: 10.14356/kona.2021005.
[48] G. Flamant *et al.*, "Solar processing of reactive particles up to 900°C, the SOLPART project," Santiago, Chile, 2018, p. 020004. doi: 10.1063/1.5067013.
[49] "Attachment_0-57-D2.5.pdf."
[50] P. E. International, "Pushing the steam cycle boundaries," *Power Engineering International*, Apr. 01, 2012. https://www.powerengineeringint.com/coal-fired/pushing-the-steam-cycle-boundaries/ (accessed Aug. 13, 2020).
[51] Y. Ahn *et al.*, "Review of supercritical CO2 power cycle technology and current status of research and development," *Nucl. Eng. Technol.*, vol. 47, no. 6, pp. 647–661, Oct. 2015, doi: 10.1016/j.net.2015.06.009.
[52] P. E. Sánchez Jiménez, A. Perejón, M. Benítez Guerrero, J. M. Valverde, C. Ortiz, and L. A. Pérez Maqueda, "High-performance and low-cost macroporous calcium oxide based materials for thermochemical energy storage in concentrated solar power plants," *Appl. Energy*, vol. 235, pp. 543–552, Feb. 2019, doi: 10.1016/j.apenergy.2018.10.131.
[53] Kyaw Kyaw, Hitoki Matsuda, and Masanobu Hasatani, "Applicability of Carbonation/Decarbonation Reactions to High-Temperature Thermal Energy Storage and Temperature Upgrading," *J. Chem. Eng. Jpn.*, vol. 29, pp. 119–125, 1996.

[54] C. Prieto, P. Cooper, A. I. Fernández, and L. F. Cabeza, “Review of technology: Thermochemical energy storage for concentrated solar power plants,” *Renew. Sustain. Energy Rev.*, vol. 60, pp. 909–929, Jul. 2016, doi: 10.1016/j.rser.2015.12.364.
[55] B. Sarrion, J. M. Valverde, A. Perejon, L. Perez-Maqueda, and P. E. Sanchez-Jimenez, “On the Multicycle Activity of Natural Limestone/Dolomite for Thermochemical Energy Storage of Concentrated Solar Power,” *Energy Technol.*, vol. 4, no. 8, pp. 1013–1019, Aug. 2016, doi: 10.1002/ente.201600068.
[56] C. Ortiz, J. M. Valverde, R. Chacartegui, L. A. Perez-Maqueda, and P. Giménez, “The Calcium-Looping (CaCO3/CaO) process for thermochemical energy storage in Concentrating Solar Power plants,” *Renew. Sustain. Energy Rev.*, vol. 113, p. 109252, Oct. 2019, doi: 10.1016/j.rser.2019.109252.
[57] S. Champagne, D. Y. Lu, R. T. Symonds, A. Macchi, and E. J. Anthony, “The effect of steam addition to the calciner in a calcium looping pilot plant,” *Powder Technol.*, vol. 290, pp. 114–123, Mar. 2016, doi: 10.1016/j.powtec.2015.07.039.
[58] M. Helbig, J. Hilz, M. Haaf, A. Daikeler, J. Ströhle, and B. Epple, “Long-term Carbonate Looping Testing in a 1 MWth Pilot Plant with Hard Coal and Lignite,” *Energy Procedia*, vol. 114, pp. 179–190, Jul. 2017, doi: 10.1016/j.egypro.2017.03.1160.
[59] Frank P. Incropera, David P. DeWitt, Theodore L. Bergman, and Adrienne S. Lavine, “Fundamentals of Heat and Mass Transfer.” Wiley, 2007.
[60] “Socratces Project Competitive & Sustainable Concentrated Solar Plants,” *Socratces Project*. https://socratces.eu/the-project/ (accessed Jun. 04, 2021).
[61] “1523643.pdf.”
[62] Ryan Melsert, Santosh Kumar Gangwal, and Tim A. Hansen, “High Temperature Thermochemical Energy Storage System,” US 10,464,815 B2
[63] H. Scott Matthews, Chris T. Hendrickson, and Deanna H. Matthews, “Life Cycle Assessment: Quantitative Approaches for Decisions that Matter.” 2014. [Online]. Available: https://www.lcatextbook.com/
[64] J. Gaede and I. H. Rowlands, “How ‘transformative’ is energy storage? Insights from stakeholder perceptions in Ontario,” *Energy Res. Soc. Sci.*, vol. 44, pp. 268–277, Oct. 2018, doi: 10.1016/j.erss.2018.05.030.
[65] C. A. Miller, A. Iles, and C. F. Jones, “The Social Dimensions of Energy Transitions,” *Sci. Cult.*, vol. 22, no. 2, pp. 135–148, Jun. 2013, doi: 10.1080/09505431.2013.786989.
[66] S. Ganowski, J. Gaede, and I. H. Rowlands, “Hot off the press! A comparative media analysis of energy storage framing in Canadian newspapers,” *Energy Res. Soc. Sci.*, vol. 46, pp. 155–168, Dec. 2018, doi: 10.1016/j.erss.2018.06.011.
[67] A. Tuck, Q. Wang, K. Malek, Y. Grinberg, and F. Bensebaa, “Canadian energy storage roadmap: terms of reference,” National Research Council of Canada. Energy, Mining and Environment, Jan. 2017. doi: 10.4224/23001380.
[68] W. Leiss and P. Larkin, “Risk communication and public engagement in CCS projects: the foundations of public acceptability,” *Int. J. Risk Assess. Manag.*, vol. 22, no. 3/4, p. 384, 2019, doi: 10.1504/IJRAM.2019.103339.
[69] S. Vercelli, J. Anderlucci, R. Memoli, N. Battisti, L. Mabon, and S. Lombardi, “Informing People about CCS: A Review of Social Research Studies,” *Energy Procedia*, vol. 37, pp. 7464–7473, 2013, doi: 10.1016/j.egypro.2013.06.690.
[70] P. Ashworth *et al.*, “Public Preferences to CCS: How does it Change Across Countries?,” *Energy Procedia*, vol. 37, pp. 7410–7418, 2013, doi: 10.1016/j.egypro.2013.06.683.
[71] S. L’Orange Seigo, J. Arvai, S. Dohle, and M. Siegrist, “Predictors of risk and benefit perception of carbon capture and storage (CCS) in regions with different stages of deployment,” *Int. J. Greenh. Gas Control*, vol. 25, pp. 23–32, Jun. 2014, doi: 10.1016/j.ijggc.2014.03.007.